D1.1: Consolidated state of the art survey and individual research proposal

Project Name: Future Networks for Innovation Research and Experimentation
Acronym: ONFIRE
Project no.: 765275

Start date of project: 01/10/2017 **Duration:** 42 Months

This project has received funding from the European Union's Horizon 2020 research and innovation programme under the Marie Skłodowska-Curie Actions.

Document Properties

Document ID	EU-H2020-MSCA-ITN-2017-765275-ONFIRE-D1.1
Document Title	*D1.1 – Consolidated state of the art survey and individual research proposal of ESR1*
Contractual date of delivery to REA	*31 July 2018*
Lead Beneficiary	Centre Tecnològic de Telecomunicacion de Catalunya (CTTC)
Editor(s)	Fabiano Locatelli (ESR1)
Work Package No.	1
Work Package Title	Disaggregated optical networks
Nature	Report
Number of Pages	50
Dissemination Level	PUBLIC
Contributors	CTTC: Josep Maria Fabrega, Michela Svaluto Moreolo NOKIA: Kostas Christodoulopoulos, Fred Buchali UPC: Salvatore Spadaro
Version Nr.	6

Executive summary

In this document, the state of the art of three main subject is presented: i) low-margin optical networks, ii) optical signal to noise ratio (OSNR) monitoring, and iii) disaggregated networks paradigm. Given the fact that the topics listed above are highly related to each other, the report outlines the connections occurring between them, which give birth to a new data-plane architecture. The objectives and the expected results of ESR1 in WP1 are discussed at the end of the document.

Contents

List of Figures

1 INTRODUCTION

1.1 DOCUMENT OBJECTIVES AND STRUCTURE

This report is intended to give an in-depth view of the data plane technologies for disaggregated optical networks. The state of the art of the subjects is provided, whose purpose is to enable the identification of open problems and methods that could be lead to the ONFIRE goals.

The document is organized as follows. Section 2 presents a deep revision of the state of the art in low-margin optical networks, explaining their principles and the techniques currently used, or under investigation, that could help their improvement.

In section 3, the state of the art in OSNR monitoring is presented. Various OSNR monitoring techniques are explained in detail together with their physical fundamentals, their possible limitations and eventually the methods to overcome these constrains.

Section 4 contains the state of the art in the disaggregated networks paradigm. The white boxes model is outlined and three possible networks visions, in which the telecommunication operators are involved in different depths, are presented.

The relation between the three main topics investigated in this report is emphasized during the whole document.

Section 5 outlines the main goals of the ONFIRE project concerning WP1 and the corresponding results expected at the end of the program, while Section 6 gives an overview of the methodology and the planning that will be followed during the Ph.D. studies.

2 LOW-MARGIN OPTICAL NETWORKS

Pointurier in [1], explains the mandatory nature of the margins, which are demanded both by operators, who have to guarantee proper operation of the network, and by network equipment providers, who have to guarantee that the network will meet specific service level agreements (SLAs). Margins should ensure the correct operations of the network in the event of degradation or aging of its elements and typically take values of several dB (e.g. 3-4 dB). In the optical layer, the margin of a lightpath is assessed as the difference between the actual quality of transmission (QoT) metric of the signal and the threshold above which the signal is considered recoverable without errors (i.e. FEC limit).

Nowadays, several vendors, conscious of the evolution towards a constantly evolving on-demand world (i.e. a scenario where the old, static network is overtaken by a new one where the bandwidth demands are continuously changing), are adopting measures to fulfil the low-margin networks paradigm that can yield significant cost savings [2]. Ciena, for example, via its *Liquid Spectrum* approach [3], is trying to make scalable, open and programmable optical networks to cope with the new dynamic and fluid bandwidth demands. According to Ciena's approach, the margins available in the optical networks can be borrowed to temporarily increase the network capacity via software and flexibly move capacity where it is needed. Other vendors that are trying to develop similar solutions for an accurate and real-time delivery of margins values are, for example, Coriant and Fujitsu. The first, by means of its *Coriant Aware Technology* [4], is trying to enhance the awareness of the optical networks' margins, thus improving the power level setting. The Coriant Aware Technology, is based on two inter-operating key elements: the Margin Processing Engine (MPE), which delivers accurate and real-time margin values, and the Optical Performance Engine (OPE), which based on the current state of the network and on the margin values coming from the MPE, provides input for the optical link control to optimally set the power levels. On the other hand, Fujitsu, proposes a conscious optical network approach [5], where the automation of the physical properties monitoring and optimum control is achieved through the use of Fujitsu's proprietary light probe technology.

As proposed in [6] three types of margins can be defined: unallocated margins (U-margins), design margins (D-margins) and system margins (S-margins). The former (i.e. **U-margins**) are known before the network deployment and come from the mismatch between the demanded capacity and reach (source-destination distance) demand, and the equipment capability (e.g. when the transponder capacity exceeds the demand at the specific reach). As pointed out in [1], the relation between data rate and reach is dictated by physics, therefore given a demand (combination of data rate and reach) and since transponders cannot transmit exactly a requested data rate over a requested reach, U-margins are unavoidable. On the other hand, **D-margins** are defined as the difference between the planned and the real performance of the deployed network; they typically take into account the uncertainties due to inaccuracies of the design tools used to evaluate the QoT and the inaccuracies of the inputs of this QoT tool. Unlike the U-margins case, their impact is only known at deployment time. Finally, the **S-margins** take into account various impairments and line degradation, such as polarization effects (a fast-varying impairment), increasing nonlinearities (network utilization is light at the beginning of its life and increase as more connections are established) and network elements aging (e.g. transponder aging, amplifier noise factor aging, fiber aging, etc.); both of the latter two factors

are considered as slow-varying impairments. Furthermore, S-margins also may include an additional arbitrary operator margin [6]. Likewise D-margins, S-margins are only known after network deployment and unlike both the other two margins types, they may vary with time. Fig.1, reproduced from [1], shows the margins' evolution over the network lifetime (i.e. starting from the network's beginning of life –BoL- and ending at the network's end of life –EoL-).

Of course, when too large, the margins provisioned during the network deployment or when a new lightpath is deployed (i.e. green field and brown field, respectively) can significantly shorten the transmission reach of the channels [7]. So they can require the use of more robust transponders or the placement of regenerators that are not needed at the time of the provisioning.

To increase the efficiency of the network the margins should be minimized by reducing or leveraging in a positive way their impact on the network. A key element to practically lower the margins is to obtain a better knowledge of the network's actual physical state: real-time monitoring techniques and an active control plane are essential to provide information about the actual state of the network and, thus, to understand the available margins, but also identify and fix any problems, if they appear by the reduction of the margins. Furthermore, thanks to coherent receivers, vastly deployed nowadays, it is possible to obtain physical layer impairments monitoring information directly by the transponders and use it at the network level for optimization purposes [8].

The main margin reduction techniques for each of the groups described above will be presented in the following subsections.

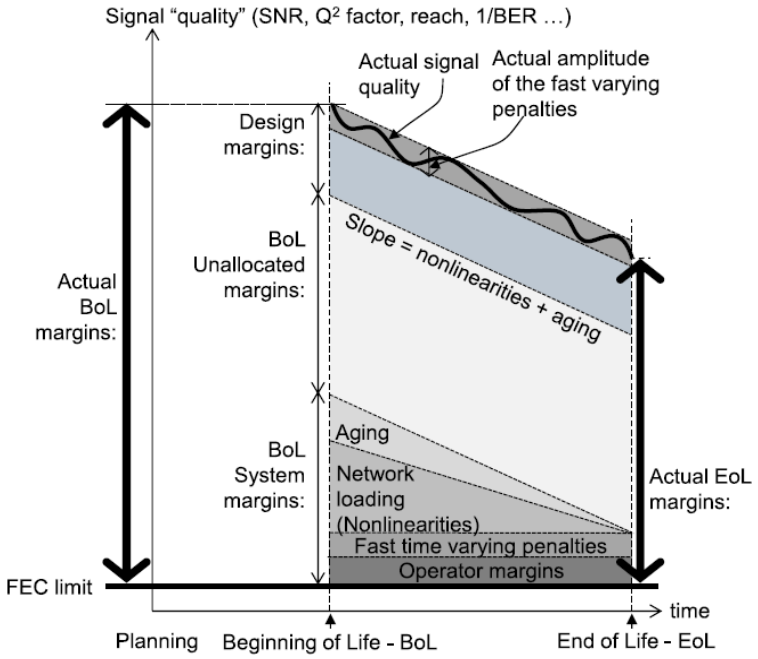

Fig. 1 Margin evolution over network lifetime. Reproduced from [1].

2.1 UNALLOCATED MARGINS REDUCTION

Even if U-margins have been previously defined as unavoidable, still their reduction can be achieved using rate-flexible transponders (flex-TRX) [1], which are devices able to adjust their capacity per wavelength depending on the existing distance and system margins [9]. U-margins can be represented by the extra capacity available in the network, which can be exploited in case of traffic demand growth simply changing the modulation format of the optical flex-TRX, as depicted in Fig.2. In such a case, U-margins can be leveraged to decrease the total cost of ownership of the network over many years.
Of course, the employment of finer granularity flex-TRX, allows the exploitation of larger U-margins' portions. To enable these finer granularities, some new techniques are currently under investigation: Probabilistic Constellation Shaping (PCS) for optical systems [10], for example, is a novel modulation approach which uses quadrature amplitude modulation (QAM) formats to achieve higher transmission capacity reach over channels. PCS modifies the symbol probability with which constellation points are used: symbols of less energy (that, on average, are more resilient to noise and other impairments) occur more frequently than symbols of higher energy. One way to implement probabilistic shaping is to assign lower number of bits to symbols having lower energy, in such a way that high energy symbols become less frequent [11]. Experimental results in [12], shows a 40% growth in the maximum transmission reach when using a system based on probabilistically shaped 64-QAM modulation formats. Another approach to improve the spectral efficiency and thus enable finer granularities flex-TRX, is the time-frequency packing (TFP) technique [13], in which a controlled interference is introduced by reducing the spacing, in both time and frequency domains, between adjacent signals.
U-margins may also be reduced by using them in restoration scenarios: in case of optical link failures, the flex-TRX is able to vary its data rate thereby exploiting the pre-planned backup path to transmit both the original traffic flow and the best effort traffic. In this way, the loss of best effort traffic can be minimized.

2.2 DESIGN MARGINS REDUCTION

As previously mentioned, D-margins are the result of the uncertainties caused by lacks of knowledge of the network topology at the time the new optical network is planned. Further uncertainties may be added during the reach calculation by the QoT estimators [14]. Indeed, network designers add significant pre-defined D-margins to the values predicted by the QoT tool to ensure that all traffic demands fulfil their target capacities. Therefore, to reduce D-margins, the development of more accurate network deployment models as well as the development of better monitoring techniques is crucial. There are two main approaches in which QoT estimation can be carried out, one based on machine learning and another one based on model of propagation physics [15]. Seve *et al*. in [15], propose an approach in which both the two previous methods are considered: the uncertainty of the input parameters of any QoT model are minimized by feeding a learning process with a set of measured/monitored data.
To improve the SNR estimation given by a QoT estimator for new lightpaths, SNR measurements from coherent receivers, terminating previously established lightpaths, have been used. The study has been carried out for a European backbone network and in Fig.3

the results regarding the error probability on the SNR prediction with and without the learning process are reported: the benefits introduced by the learning process are easily observable by the reduction of the SNR error distribution width. Another example of how the usage of QoT monitoring data, as optimization starting point, can lead to uncertainties reduction of input data of the QoT tool (i.e. to D-margins reduction), is proposed in [16]. In this paper, the authors correlates the monitored QoT values of established lightpaths to estimate the QoT of new lightpaths. As the network evolves, more information are available and the estimated QoT becomes more accurate.

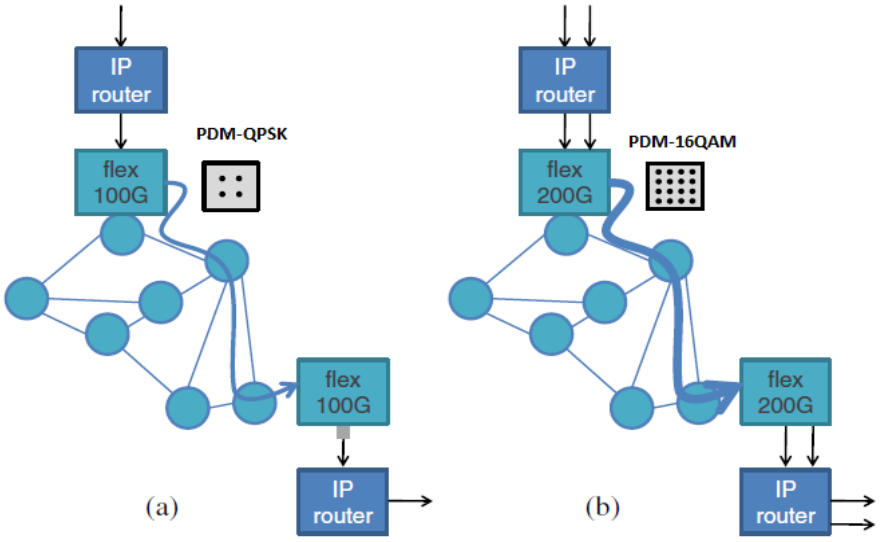

Fig. 2 Network upgrade as a result of traffic growth: when more capacity is needed the modulation format is changed. Reproduced from [1].

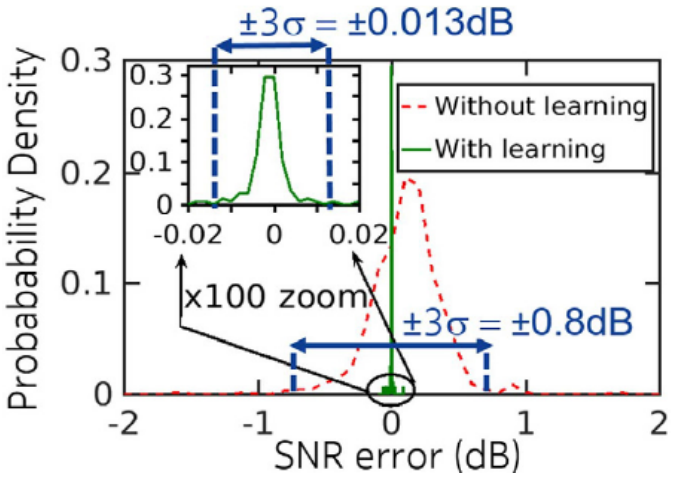

Fig. 3 Probability density of the SNR prediction error with (solid green line) and without (dashed red line) learning process. For these results to be collected, the learning process has been applied on a semi-analytical model for brisk assessment (SAMBA) of performance. Reproduced from [15].

2.3 SYSTEM MARGINS REDUCTION

As explained in [1], the reduction of S-margins is basically related to an RMSPA (routing, modulation, spectrum and power allocation) network design problem: each lightpath has to be optimized with the best modulation format, power and spectrum to accommodate more capacity in the network. For instance, dynamic modulation format control can be a way to reduce system margins by adjusting to lower order modulation format any link degrading the signal [17].
In this direction, [7], exploits the usage of elastic optical transponders to dynamically fit the progressive ageing of optical transmission links. Following the progressive link margins paradigm, the equipment must be used at the maximum capacity during the network BoL (i.e. the moment where S-margins are greater), while as the network elements age and the nonlinearities grow (because of the grown load of traffic in the network during its lifetime) the margin should decrease together with the network capacity. Postponing the purchase of new equipment means lower the costs and gradually upgrading the network: indeed as the time advances, more advanced equipment are developed and are available at cheaper prices. Of course, as already mentioned, this approach would give better results if used in presence of advanced monitoring techniques.
In [2], Soumplis *et al*., modelled the degradation introduced by the network components ageing and proposed an economic cost model to quantify the benefits of postponing the equipment's purchase. Besides that, the authors proposed a heuristic routing and spectrum allocation (RSA) algorithm that optimizes the decisions regarding the placement and the transmission parameters of configurable transponders, based on the measured physical layer conditions (in the work this solution is referred as "actual margins"). Using the proposed algorithm, a large cost saving of almost 36% is achievable for an elastic network (considering also optimized launch power), compared with a scenario that uses worst-case margins. In Fig.4 the accumulated total costs for an elastic network are shown: as expected the actual margin outperforms all the other considered cases.

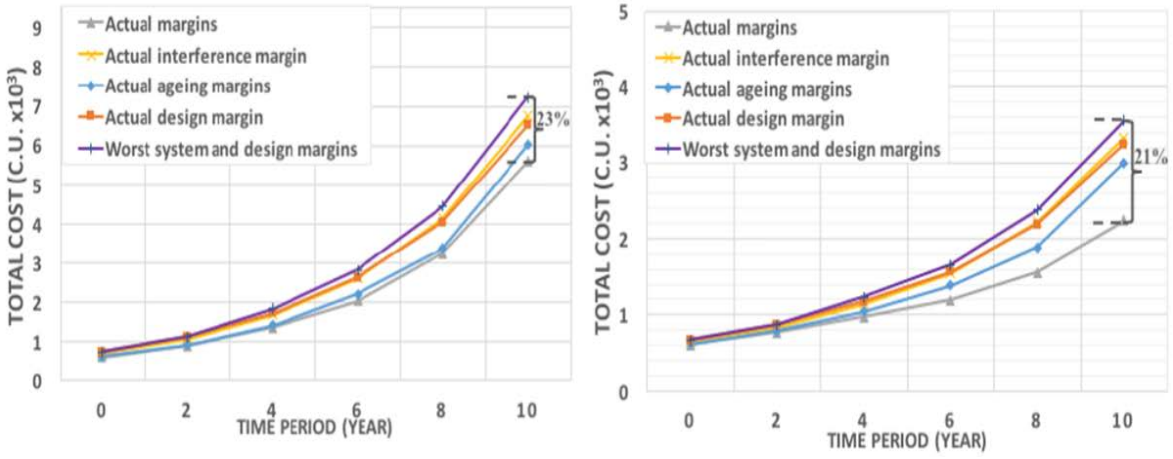

Fig. 4 Accumulated total costs, in C.U. (1 cost unit is defined as the cost of the 100 Gpbs transponder), for the multi-period incremental planning of an elastic network. Left figure assumes price projection A for the network equipment, while the right one price projection B. Both the price projection tables can be found as Table 2 at page 6 of [2]**. Reproduced from** [2]**.**

An approach based on cognitive science, in particular exploiting the case-based reasoning (CBR) technique, has been proposed in [18]. In this paper, the authors, considered the S-margins as variable over time (i.e. lower at the BoL and higher when optical infrastructure ages and degrades) and set their values based on the results of the cognitive technique, which also take into account the long-term aging process of the components. Therefore, the S-margins values of the current lightpaths are modelled on the past ones established for the same paths. Thanks to the application of this technique, the authors were able to save power up to 1.31dB, representing a 53% improvement of the preassigned mean transmitted power.

2.4 SOFT FAILURES

Operating the optical networks close to the margin-less region, involves not only the benefits mentioned in the previous subsection, but also situations in which the reserved margins could not be enough to guarantee an error-free transmission. Indeed, if some natural performance variations occur (e.g. due to polarization effects, network loading or network's elements ageing), the bit error ratio (BER) threshold could be exceeded, and soft-failures (SF) could appear [19]. SF are defined as failures, faults, defects or errors that result in a temporary system stoppage, and that can be fixed by means of a system hardware reset, software performance reset, or a non-repair maintenance action [20]. Therefore, if QoT degrades due to SF presence, some measure need to be adopted to adjust the problems, avoiding SLA violations.

In [21], the authors demonstrate a self-healing elastic optical network (EON), achieved following the *observe-decide-act* paradigm (depicted in Fig.5), where coherent receivers are exploited as software defined optical performance monitors (soft-OPMs) and their feedback allows to localize and handle SFs. As already pointed out several times before, even in this case, a crucial role is played by the network's ability of monitoring its performance at the physical layer. Once the monitoring information (e.g. pre-forward error correction-BER, OSNR, etc.) is collected by the soft-OPMs ("*observation*" phase), it is transferred to the management plane where the application-based network operations (ABNO) controller [22], by means of a path computation element (PCE), will decide what action to take ("*decision*" phase). Depending on the traffic's class of service, the reconfiguration steps to follow in the event of SFs, are different: in case of gold connections, the full bit rate has to be maintained, while in the bronze connections case, the full bit rate can be modified. In both cases, the taken decisions correspond to a format and code rate adaptation. Finally, the ABNO controller reconfigure the data plane to restore the service ("*action*" phase).

A machine learning (ML)-based BER prediction approach, has been leveraged by Delezoide *et al*. in [19], to demonstrate the functioning of a minimal margins network subjected to ageing and short-term performance fluctuations. In this paper, the authors have been able to automatic adapt the optical connections to the ageing of different elements: under fiber/amplifier ageing condition, the SDN-based optical testbed dynamically adapted the capacity according to the available margins, while under filter ageing condi-

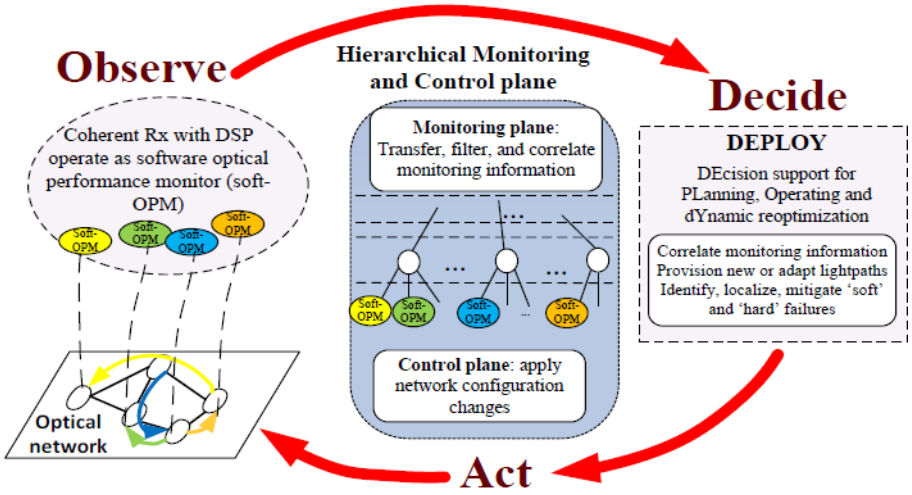

Fig. 5 Observe-decide-act control loop scheme. Reproduced from [21].

tion a filter-aware BER prediction has been carried out. Also in this work, as for [21], the control plane has been managed by the ORCHESTRA's infrastructure [22].

Localization of SFs in EONs, has been investigated in [23], for two different kind of scenario: during the customer lightpath commissioning testing phase, in which the lightpath's performance must be checked before the final delivery, and during the effective operation of the lightpath. For the former case, the authors proposed an evolution of the optical supervisory channel (OSC) technique, named optical testing channel (OTC), where instead of using a high-speed coherent signal for the low-speed low-index on-off keying (OOK) modulation, a continuous-wave laser has been adopted. On the other hand, for the in-operation case, optical spectrum analyzers (OSAs) have been placed in every outgoing link of the test network. While with the OTCs an active monitoring is carried out injecting a test signal in the network, OSAs presence involve passive monitoring also to facilitate lightpath rerouting. In Fig.6, the described node architecture is depicted. Both the two previous techniques have been demonstrated and validated by means of simulations that showed how these approaches can estimate the BER in an accurate way.

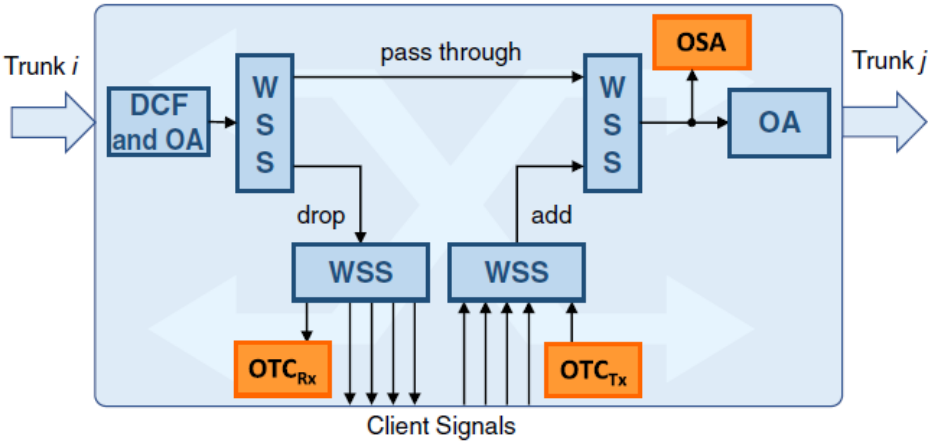

Fig. 6 Optical node architecture diagram with OTCs and OSA. Reproduced from [23].

3 OPTICAL SIGNAL-TO-NOISE RATIO MONITORING

As observed in the low-margin optical networks state of the art, the optical performance monitoring (OPM) techniques assume a crucial role in the evolution towards more intelligent and self-aware optical networks. A real-time network parameters monitor is needed to collect the information that the network will process in order to take new decisions. Since the OSNR is transparent to both the bit-rate and the modulation format and is directly correlated to the BER [24], it has become one of the most important parameter to be monitored in the optical layer. Thus, this section aims to give a complete review of the current state of the art of the OSNR monitoring techniques.

Optical amplifiers have assumed a crucial role to compensate the fiber losses in optical networks, thus an accurate analysis of their contribution in terms of noise is needed. Indeed, when an optical amplifier amplifies a signal, it also adds undesired noise due to amplified spontaneous emission (ASE). ASE affects the receiver ability to properly decode the optical signal and thus introduces errors. ASE can be quantified in terms of OSNR as [24]:

$$OSNR = \frac{P_s}{P_n} + \frac{B_m}{B_r}$$

where:

- P_s represents the power of the optical signal
- P_n represents the power of the optical noise
- B_m represents the noise equivalent bandwidth (NEB) of the OSA
- B_r represents the measured resolution bandwidth (RBW)

OSNR can be graphically represented as depicted in Fig.7. In the following sections, the main OSNR monitoring techniques are listed and a brief explanation of each approach, with its limitations and some possible way to overcome them, is given.

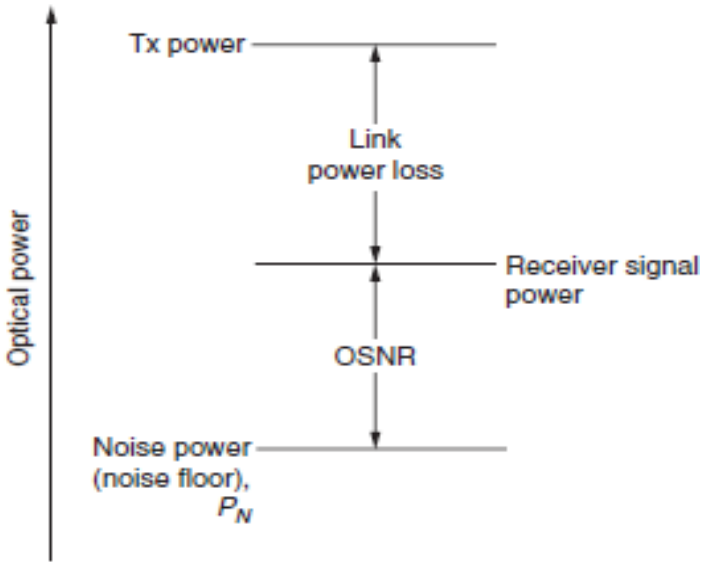

Fig. 7 OSNR diagram. Reproduced from [24]**.**

3.1 LINEAR INTERPOLATION (LI) TECHNIQUES

3.1.1 OPTICAL SPECTRUM ANALYSIS TECHNIQUE

Assumption: the ASE noise optical spectrum is assumed to be almost uniform [25].

The noise level of each peak of the optical spectrum (each peak corresponds to the operating wavelength of each wavelength-division multiplexed –WDM- channel) is estimated interpolating the noise power levels measured at the two adjacent peaks. In Fig.8, the OSA operating scheme is shown. The resolution bandwidth of this technique (i.e. OSA resolution bandwidth) is assumed to be the bandwidth of the filter used to slice the ASE noise. In general the power levels of the WDM signals are not so sensitive to the OSA resolution bandwidth, while the ASE noise power level is strongly dependent to it. The measured OSNR is then inversely proportional to the resolution bandwidth of the OSA.

3.1.2 OUT-OF-BAND NOISE MEASUREMENTS TECHNIQUE

Assumption: Optical spectrum of the ASE noise assumed as flat and wide [25].

The noise levels of each wavelength are estimated measuring the noise power level at an out-of-band wavelength. The measurements can be done by mean of an arrayed waveguide grating (AWG) as shown in Fig.9, or by mean of OSAs.

3.1.3 LI TECHNIQUES POTENTIAL PROBLEMS

- In a dynamically reconfigurable transparent optical networking scenario, the spectrum of the ASE noise can be different at each wavelength (see Fig.10) resulting in large OSNR error measurements when analyzed with LI techniques. This problem can be overcome employing high-resolution optical spectrum analysis.
- If the transmission involves high-speed phase modulated signals with dense channel spacing, the signals' spectral power is distributed like the ASE noises.

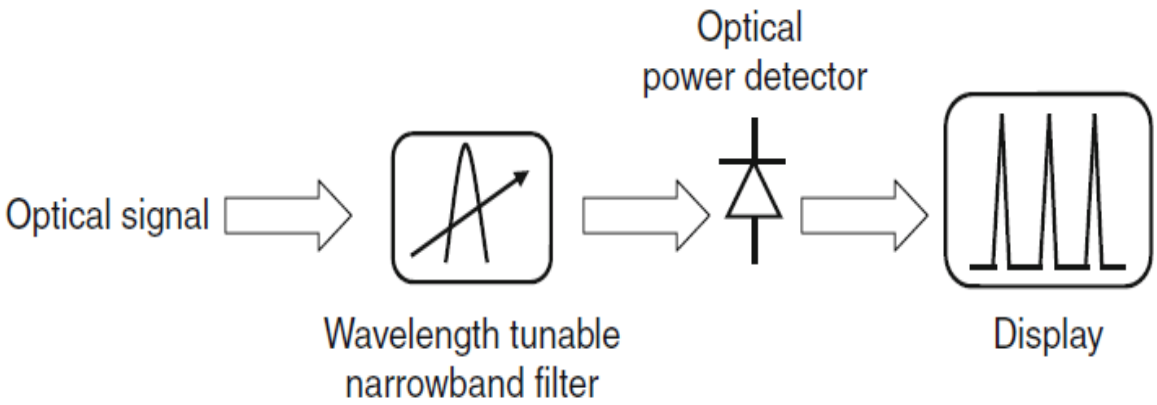

Fig. 8 Optical spectrum analyzer (OSA) operating scheme. Reproduced from [25].

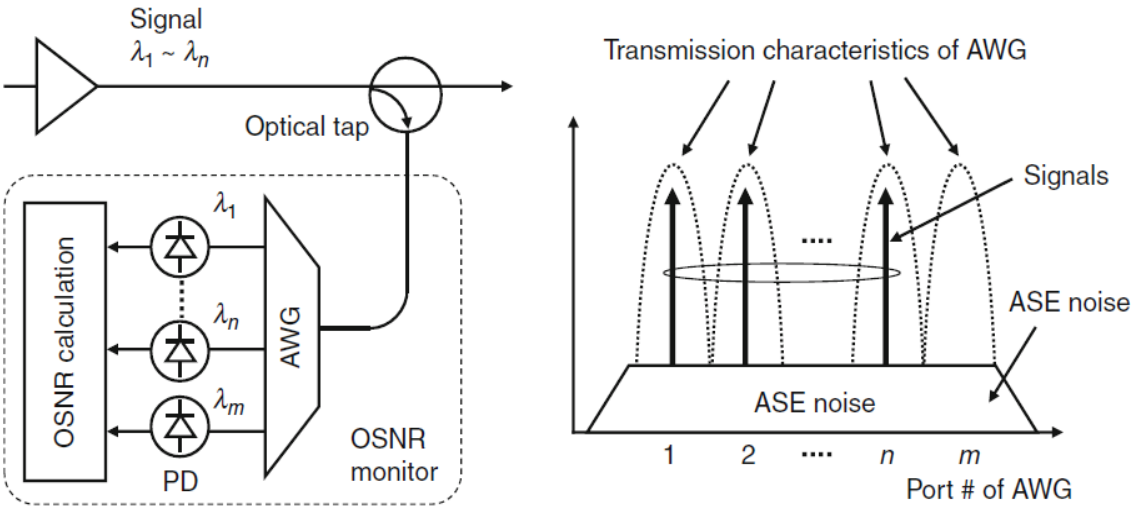

Fig. 9 Out-of-band noise measurement using an AWG: λ_m represents the out-of-band wavelength. Reproduced from [25].

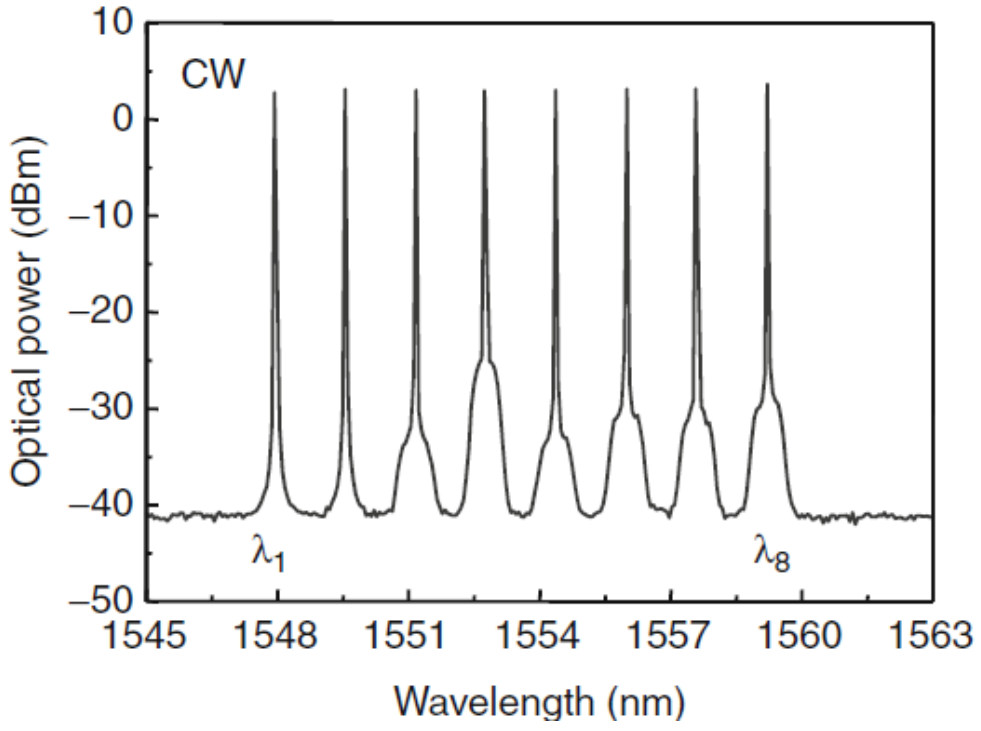

Fig. 10 Optical spectrum of unmodulated continuous waveform signals with eight wavelength channels. It is easily observable how the ASE noise levels vary with the wavelength. Reproduced from [25].

3.2 POLARIZATION-BASED (PB) TECHNIQUES

Assumption: ASE noise is completely depolarized, i.e. have an even power distribution for every polarization direction, while usually an optical signal features a high degree of polarization, containing the entire power in a precise polarization state [25]. Polarization multiplexed signals, which transmit information on two orthogonal polarization states, do not meet this condition and therefore are not suitable for this technique.

3.2.1 POLARIZATION NULLING TECHNIQUE

Assumption: a polarization controller (PC) is not able to confer any changes upon the polarization state of depolarized signal like ASE noise [26].

This technique is implemented by feeding a PC with an arbitrarily polarized optical signal and the completely depolarized ASE noise. Due to the polarization nature of the signals, the PC will commute the first one into a linearly polarized signal while the ASE noise will maintain its depolarized state. Using two orthogonally aligned linear polarizers, the mixture is then split into two orthogonal polarization components: the first one (i.e. the one aligned with the signal's polarization direction) will contain both the power of the optical signal and the power of the polarized ASE noise, while the second one (i.e. the component aligned with the orthogonal state of the signal's polarization direction) will be composed just by the polarized ASE noise (i.e. the noise part featuring that precise state of polarization). The scheme of the PB technique is depicted in Fig.11.

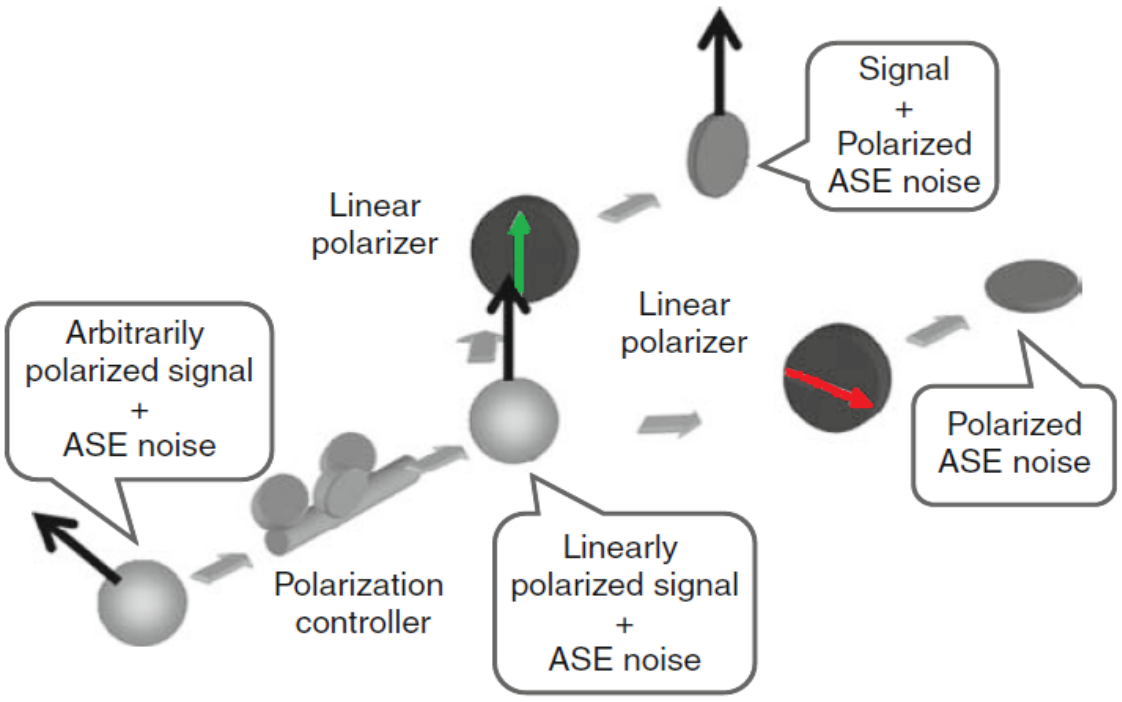

Fig. 11 Polarization-nulling technique scheme. Reproduced from [26]**.**

Considering that the polarized ASE noise has a power equal to one-half of the total ASE noise, the OSNR is obtained as:

$$OSNR = \frac{P_s}{P_n}\left(\frac{B_n}{B_r}\right) = \frac{P_p - P_o}{2P_o}\left(\frac{B_n}{B_r}\right)$$

where:

- B_n represents the noise-equivalent bandwidth (determined by the passband of the channel section filter)
- B_r represents the resolution bandwidth that defines the OSNR
- P_p represents the optical power measured after the linear polarizer aligned with the signal's polarization direction
- P_o represents the optical power measured after the linear polarizer aligned with the orthogonal state of the signal's polarization direction

3.2.2 STOKES PARAMETERS ANALYSIS (SPA) TECHNIQUE

Assumption: Stokes parameters describe the polarization state of electromagnetic radiation [27]. One of them is the degree of polarization (DOP) which quantifies the polarized portion of an electromagnetic wave giving an estimation of the ASE noises' power. DOP is defined as:

$$DOP = \frac{Polarized\ light\ power}{Total\ light\ power} = \frac{P_s}{P_s + P_n}$$

The OSNR can be then expressed as [28]:

$$OSNR = \frac{DOP}{1 - DOP}$$

To properly exploit this technique a very high accuracy in the DOP measurement is needed, because as the OSNR increases the monitoring process becomes very sensitive to the DOP error.

3.2.3 PB TECHNIQUES POTENTIAL PROBLEMS

- **Polarization Mode Dispersion (PMD):** two orthogonal polarization components of an optical signal propagate in the fiber at different velocity due to imperfections of the fiber itself, which break its circular symmetry [27][29]. This results in leaks of the signal power into the orthogonal polarization state. Thus, at the polarizer aligned with the orthogonal state of the signal (i.e. the one at which just the polarized ASE noise should be measured) small components of the optical signal will be measured, resulting in monitoring errors. OSNR error caused by PMD can be described as [26]:

$$Error\ [dB] = 10log\left(\frac{OSNR_r}{OSNR_m}\right) = 10log\left[\frac{1 + 2\varepsilon_{PMD}OSNR_r}{1 - 2\varepsilon_{PMD}}\right]$$

where:
- $OSNR_r$ represents the real OSNR
- $OSNR_m$ represents the measured OSNR
- ε_{PMD} represents the fraction of the optical signal power leaked into the orthogonal polarization state from the signal's polarization due to PMD

The OSNR error increases with ε_{PMD} and transmission speed as shown Fig.12a. In particular, during the execution of polarization based OSNR monitoring techniques, the monitoring error caused by PMD becomes non-negligible if the system is operating at speeds higher than 10 Gb/s for mid-range link distancies [30].

- **Non-linear Birefringence (NLB):** birefringence is a property of some materials for which the refractive index depends on the polarization direction [27]. Nonlinear birefringence happens when WDM signal are transmitted in the optical fiber: the polarization state of one channel (i.e. wavelength) could be affected by the intensity of the other channels. Therefore, as in the PMD case, at the polarizer aligned with the orthogonal state of polarization (SOP) of the signal, a small portion of the signal power could be included in the noise power measurements, resulting in overestimation of the noise power. OSNR error caused by NLB can be described as [26]:

$$Error\ [dB] = 10log\left[\frac{1 + 2\varepsilon_{NL}OSNR_r}{1 - 2\varepsilon_{NL}}\right]$$

where:
- ε_{NL} represents the fraction of the optical signal power leaked into the orthogonal polarization state from the signal's polarization due to NLB

The OSNR monitoring error grows as the frequency decreases, on the contrary of what happened with the PMD (see Fig.12b). Indeed, at speeds lower than 10 Gb/s, the effect of nonlinear birefringence predominates over the effect of PMD [25].

- **Polarization Dependent Loss (PDL):** it is a loss that varies as the polarization state of the propagating wave changes because of the anisotropy of the network components [27]. Due to PDL, ASE noise could be partially polarized and at the exit of the two linear polarizers (i.e. the one aligned with the signal's polarization direction and the one orthogonal to it) the amount of the two noise powers could be no longer identical (see Fig.13), resulting in a monitoring error described as

[31]:

$$Error\ [dB] = 10log[1 - DOP_{ASE}(\hat{s} \cdot \hat{n})]$$

where:
- DOP_{ASE} represents the DOP of the ASE noises
- $\hat{s}$ represents the normalized Stokes vector of the signal
- $\hat{n}$ represents the normalized Stokes vector of the partially polarized ASE noises

The effect of PDL on the monitored OSNR is negligible even for ultra-long-distance transmission systems if the PDL/span is less than 0.2 dB. If ROADMs are used in the network, this level could be exceeded, and the error might be increased.

- **Polarization Fluctuations:** in some specific environmental conditions (e.g. aerial fiber link), the SOP of the optical signal could rapidly fluctuate at a certain frequency values [32], due to Faraday rotation caused by the current in the electrical power line or by the wind and the pendulum motion of the wire. Actually, current technologies can overcome these limitations by tracking the polarization at speeds fast enough to not cause errors [33].

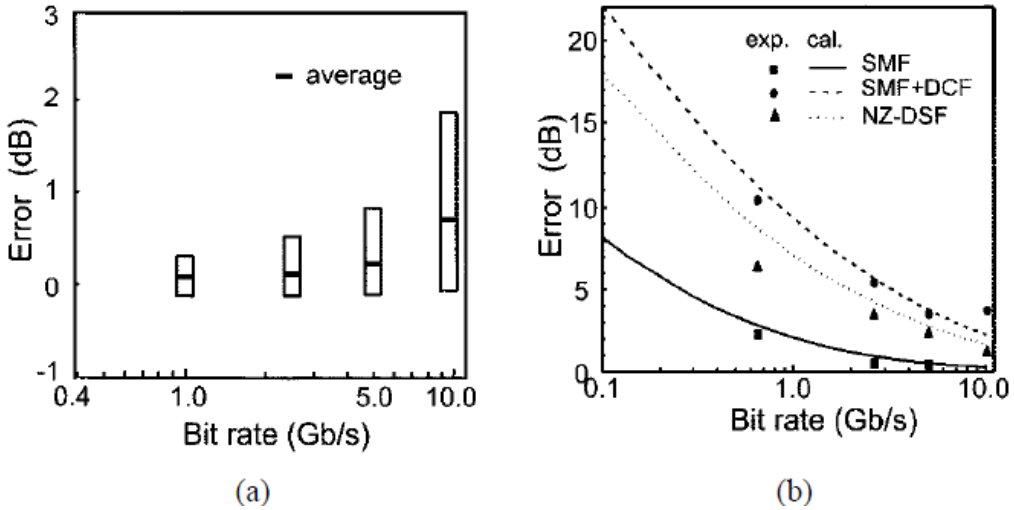

Fig. 12 OSNR monitoring error caused by (a) PMD and (b) NLB. Reproduced from [30].

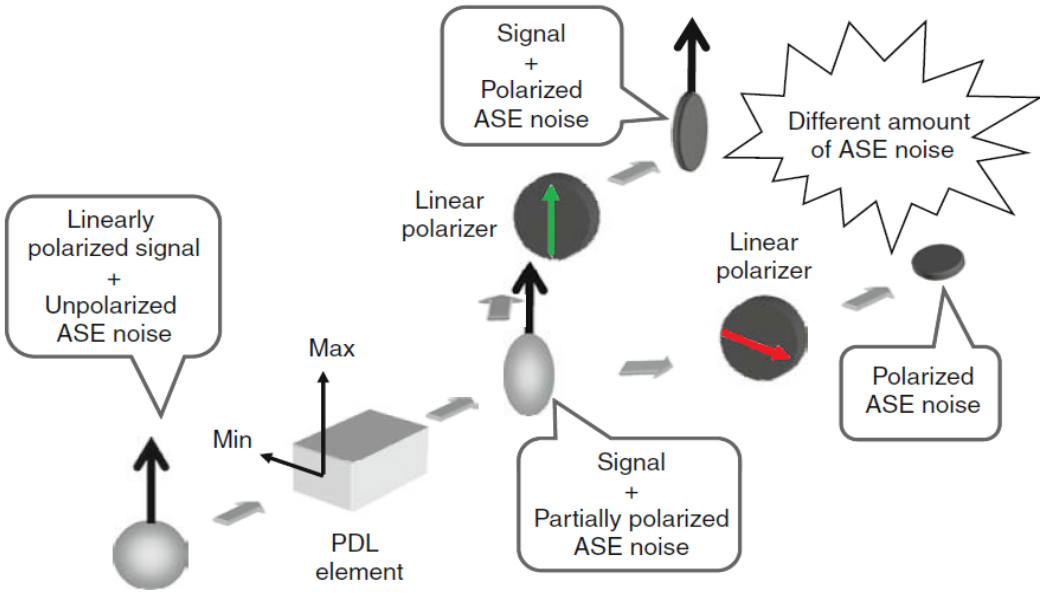

Fig. 13 Error mechanism caused by PDL. Reproduced from [25].

3.2.4 POSSIBLE METHODS TO OVERCOME LIMITATIONS

- **Additional optical filtering:** while working with the polarization-nulling technique, due to the effects of PMD and/or nonlinear birefringence, small amounts of the signal power could leak into the arm where only the noise should be measured. One approach to deal with this problem is to split the arm with the polarized ASE noise into two more arms and to add a second optical bandpass filter (BPF) to one of these two new arms. The aim of this new filter is to reduce the ASE noise bandwidth and leave just the leaked signal component that will be then subtracted to the power of the non-filtered arm, as showed in Fig.14. The OSNR of this technique is thus obtained as [34]:

$$OSNR = \frac{P_s}{P_n}\left(\frac{B_n}{B_r}\right) = \left[\frac{(P_1 + 2P_2)}{4(P_2 - P_3)/(1-\alpha)} - 1\right]\left(\frac{B_n}{B_r}\right)$$

where:

- P_1 represents the signal power in the first arm
- P_2 represents the polarized ASE noise power in the first split arm
- P_3 represents the polarized ASE noise power in the second split arm (i.e. the one filtered)
- α represents the bandwidth reduction factor determined by the transmission characteristics of the first and the second BPFs

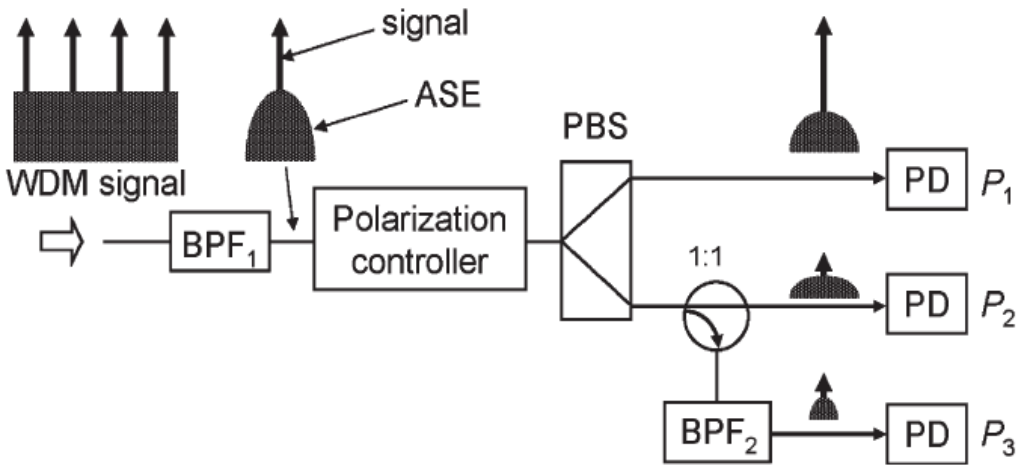

Fig. 14 Polarization-nulling technique improved by using an additional optical filter. (PBS: polarization beam splitter, BPF: bandpass filter, PD: photodetector). Reproduced from [26]**.**

Limits of this technique arise when the ASE noise has a bandwidth comparable to the one of the high-speed optical signals. This approach also requires the precise alignment of the two tuneable filters [34].

- **Off-center narrow-band filtering:** the approach presented in [35], refers to the polarization-nulling technique. Exploiting the fact that the spectral power of a modulated optical signal is sensitive to the frequency (i.e. it decreases as we move away from the center), while the ASE noises have an almost flat spectral power, the noise power can be measured at a frequency different from the centered one where the signal power is very low, as shown in Fig.15a. Indeed, the monitoring error caused by PMD decreases as the offset from the center frequency increases. In addition, the narrower the filter is, the lower it will be the PMD effect. Limits of this technique arise when the depolarization of the optical signal becomes significant [25].

- **Multiple-frequency measurements:** this approach, presented in [36], measures the noise power level at two different frequencies, assuming that the effect of nonlinear birefringence is even for all spectral components. The OSNR is estimated as:

$$OSNR = \frac{P_t - P_n B_t/B_f}{P_n B_r/B_f}$$

where:

- P_t represents the total power of the optical signal and the ASE noise within the

bandwidth B_t

- B_t represents the bandwidth within which the total power is measured
- B_f represents the bandwidth of the tuneable BPF
- P_n represents the ASE noise power

In Fig.15b, a schematic diagram of the improved polarization-nulling technique by means of multiple-frequency measurement and PMD compensation is depicted. Limits of this technique arise when the nonlinear birefringence significantly interacts with large PMD [25].

- **Spectral SOP measurement:** referring to the Stokes parameter analysis technique, in [37], a way to avoid the effect of PMD is presented: measure the SOP of the spectral components of the optical signal at multiple wavelengths with very high spectral resolution and estimate the degree of polarization of the PMD (DOP_{PMD}) from the powers. The limit of this technique is the vulnerability to the effects of nonlinear birefringence.

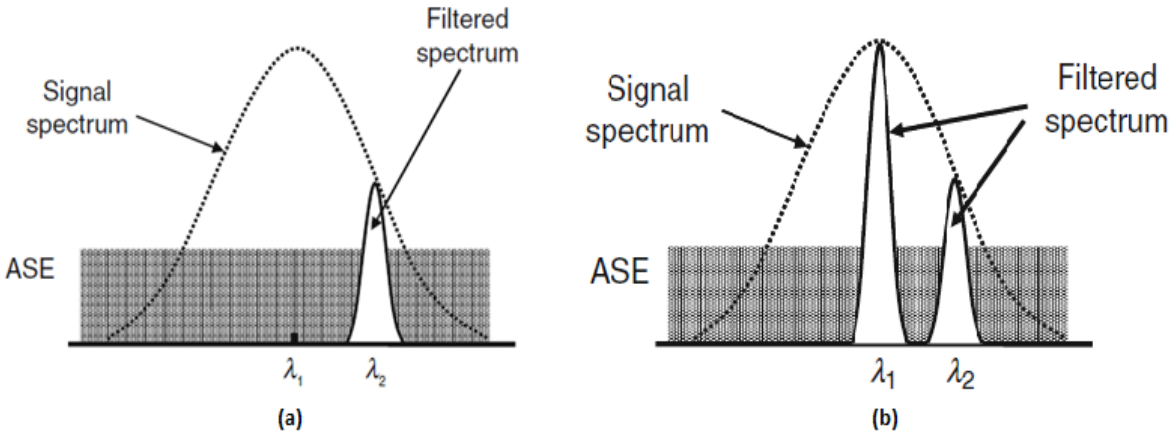

Fig. 15 (a) Illustration of the off-center filtering technique. Reproduced from [25]**. (b) Illustration of the multiple-frequency measurement technique. Reproduced from** [26]**.**

3.3 INTERFEROMETER-BASED (IB) TECHNIQUE

Assumption: the optical signal is highly coherent whereas ASE noise is incoherent [38].

This technique works thanks to a Mach-Zehnder delay interferometer (MZDI): the total power (i.e. signal power plus ASE noise power) is measured with the constructive interference (see Fig.16a), while the noise power is measured eliminating the optical signal with destructive interference (see Fig.16b). The constructive or destructive interference are achieved by means of an optical delay and a phase adjuster, contained inside the MZDI, which can tune the phase on one of the two optical paths that will be then recombined in the desired way.

This approach is insensitive to chromatic dispersion (CD) or polarization effects [39].

3.3.1 IB TECHNIQUE POTENTIAL PROBLEMS

- It is difficult to use this technique for OSNR monitoring of WDM signals with high spectral density: the destructive MZDI rejects not only the optical signal but also the ASE noises

3.3.2 POSSIBLE METHODS TO OVERCOME LIMITATIONS

A possible solution could exploit the polarization property of the ASE noises [25]. On the other hand, this method would introduce the polarization related problems explained in the previous sections, such as the sensitivity to PMD and nonlinear birefringence.

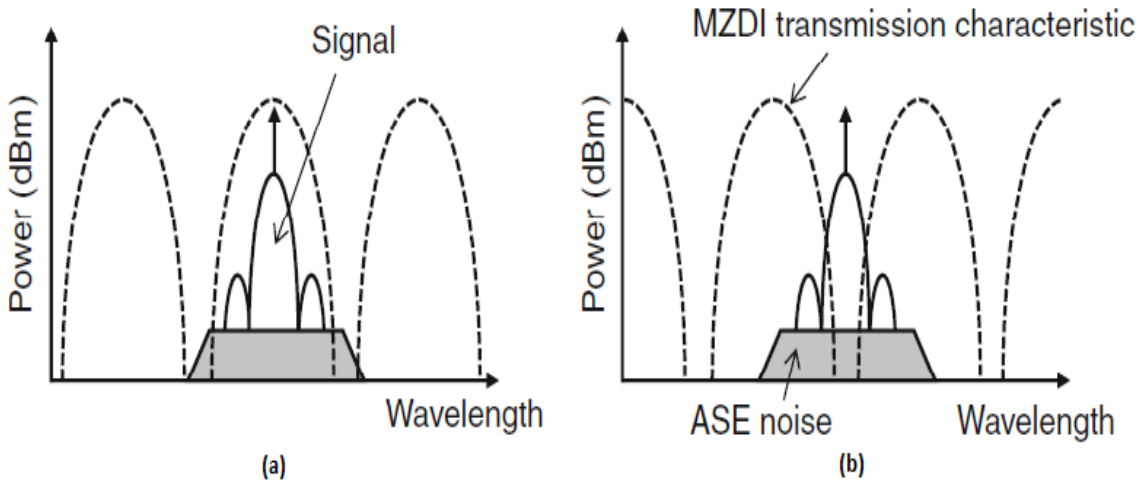

Fig. 16 (a) The total power (signal power plus noise power) is measured with constructive interference: Mach-Zehnder transmission characteristic matches the signal and the noise. (b) Destructive interference situation: MZ transmission characteristic still matches the noise but the signal shape remains outside the transmission characteristic. Reproduced from [25].

3.4 BEAT NOISE ANALYSIS (BNA) TECHNIQUES

Assumption: the receiver's dominant source of noise is caused by beating between the optical signal and the ASE noises. Thus, the receiver's electrical noise analysis becomes a possible approach for OSNR estimation [40].

Direct detection works with a square-law receiver: if the optical signal is detected together with the ASE noises, beat noises will occur. In particular, the current at the receiver output will be composed by the signal-spontaneous beat noises term (i.e. the one caused by beating between the optical signal and the ASE noises) and the spontaneous-spontaneous beat noises term (i.e. the beat noises caused by beating between among ASE noises).

In most cases, the total noise power can be approximated with the beat noises electrical power, which at low frequencies (i.e. $f \ll B_o$) can be expressed as [40]:

$$P_{beat} \approx A\left(\frac{2P_sP_n}{B_o}+\frac{P_n^2}{B_o}\right)=\frac{2AP_s^2}{B_r}\left(\frac{1}{OSNR}+\frac{B_o}{2B_r\cdot OSNR^2}\right)$$

where:
- A represents a constant
- B_o represents the optical bandwidth (i.e. the ASE noises bandwidth)
- $OSNR$ represents the OSNR of the optical signal measured with the resolution bandwidth of B_r

The total optical power is given by the sum of the signal power and the ASE noises power, that is [40]:

$$P_{total}=P_s+P_{ASE}=P_s\left(1+\frac{1}{OSNR}\frac{B_o}{B_r}\right)$$

Both P_{beat} and P_{total} are measurable, thus the OSNR can be calculated from the two previous equations. If the signal is made of repetitive bit patterns its spectrum will consists of discrete spectral components, thus an OSNR estimation could be done by measuring the beat noises' power at low frequencies [40], as shown in Fig.17a. On the other hand, the power of the beat noises can be also measured at high frequencies since the spectral density of the received signal decreases really fast after a certain frequency value [41], as shown in Fig.17b.

3.4.1 BNA TECHNIQUES POTENTIAL PROBLEMS

For what concerns the OSNR monitoring technique based on low-frequency noise analysis, the most critical problem is that real user traffic has random patterns rather than repetitive ones, so the low frequency region will not be free of signal spectrum.
Also at low-frequencies, beat noises can be caused by multipath interference (MPI) noises [25].

On the other hand, the biggest limit of the OSNR monitoring technique based on high-frequency noise analysis is the need of RF components that operate at frequencies much

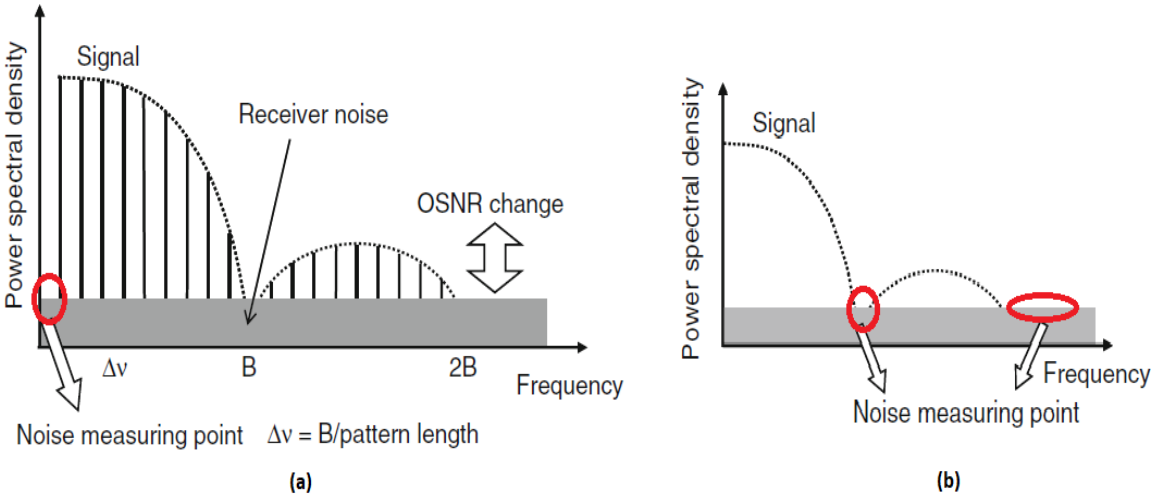

Fig. 17 OSNR monitoring technique based on: (a) low-frequency and (b) high-frequency beat-noise analysis. Reproduced from [25]**.**

higher than the bit rate, which for high-speed signals (i.e. data rate ≥ 40 Gb/s) could be a problem [25].

3.4.2 POSSIBLE METHODS TO OVERCOME LIMITATIONS

Goal: eliminate the signal spectrum in a certain frequency region without changing the noise density, to allow accurate measurements of the beat noise.

- **POLARIZATION-DIVERSITY TECHNIQUE**
  Fundamental: if a highly polarized optical signal is split into two orthogonally polarized components, the outputs' waveform will be highly correlated. On the contrary, two orthogonally polarized components of the depolarized ASE noise are completely uncorrelated in nature.

  This technique, presented in [42], consists in splitting an optical signal into two orthogonally polarized components by means of a polarization controller and a polarization beam splitter (PBS) and then detect the signals with a polarization-diversity receiver. The proposed monitor structure is depicted in Fig.18. Since the beat noises from the PDs are completely uncorrelated to each other, if the two outputs are subtracted, the signal components will be cancelled out while the beat noises will be added in terms of power.
  Measure the noises in the low-frequencies region is cost effective and allows to neglect the PMD effect. This technique is also CD insensitive.

  Limitation: during the subtraction process the polarization-diversity receiver converts polarization variation into intensity variation, thus the effect of nonlinear birefringence could cause problems especially at low frequencies [25].

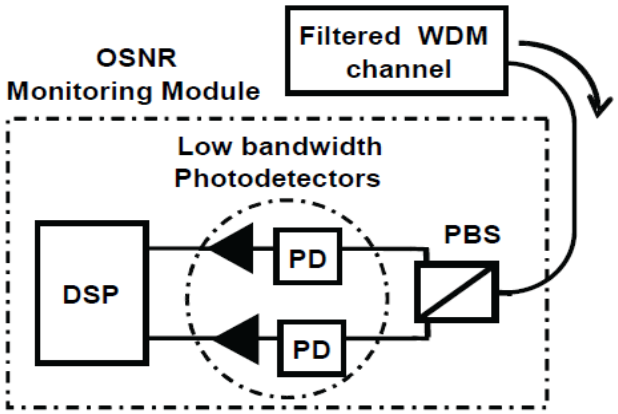

Fig. 18 Schematic diagram of the OSNR monitoring technique based on polarization-diversity method. Reproduced from [42].

- **ORTHOGONAL POLARIZATION DELAYED-HOMODYNE TECHNIQUE**
  Fundamental: this technique, presented in [43], eliminates the signal spectrum for a single frequency rather than for the entire spectrum, as shown in Fig.19.

  It consists in splitting an optical signal into two polarization components by means of a polarization controller and a PBS, delaying one of the two and recombining the signal by means of a second PBS. Using the Fourier transform the power spectral density of the received signal is found to be nullified at certain frequencies, which values can be modified changing the optical delay. This technique is robust to PMD and insensitive to CD, also at high frequencies it shows low nonlinear birefringence effects.

  Limitation: nullifying the signal spectrum at low frequencies requires a large amount of differential group delay (DGD), thus monitoring at high frequencies is preferred [25].

- **ORTHOGONAL POLARIZATION SELF-HETERODYNE TECHNIQUE**
  Fundamental: this technique, presented in [44], generates beat noise by mixing two orthogonally polarized spectral components obtained filtering the same optical signal at different frequencies.

  It consists in splitting the optical signal into two components: each one of the two get filtered by a narrow BPF centered at a different frequency so that uncorrelated ASE noise is selected. By means of a polarization controller, the spectral compon-

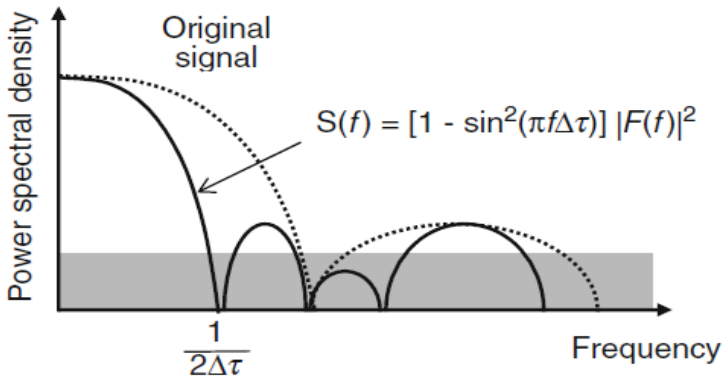

Fig. 19 Example of a nullified data spectrum using the orthogonal polarization delayed-homodyne technique. Reproduced from [25].

ents of the two branches are made orthogonal to each other and then are combined and received by a PD giving rise to beat noises around a certain frequency value. The condition to be respected that will guarantee that no signal components will arise where the beat noise has been generated regards the distance of the two BPF [44]:

$$\Delta f = |f_1 - f_2| > \left(\frac{B_2 + B_1}{2}\right)$$

This technique is immune to first-order PMD and insensitive to nonlinear birefringence. A simplified scheme of the technique's procedures is shown in Fig.20.

Limitation: the orthogonal polarization self-heterodyne approach can be sensible to higher-order PMD that can induce a different amount of depolarization on the spectral components of the two branches [25].

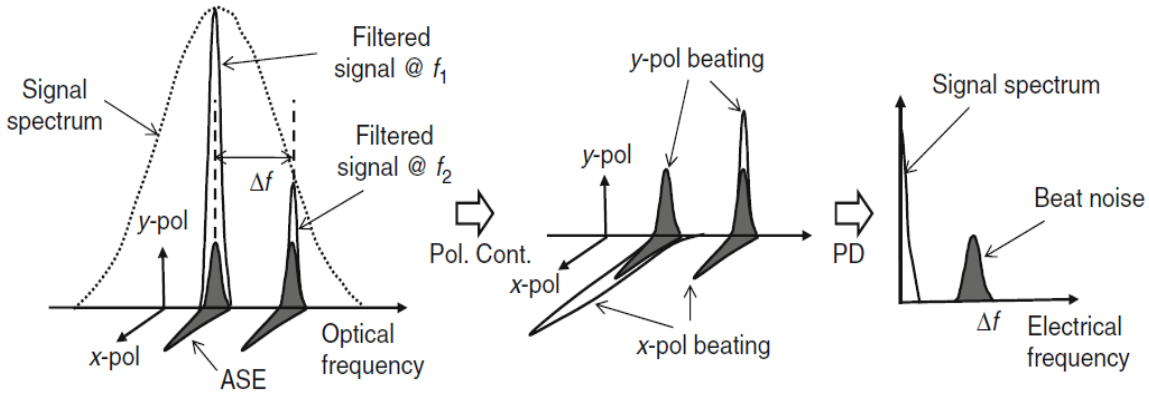

Fig. 20 Scheme of the orthogonal polarization self-heterodyne technique, where f_1 and f_2 corresponds to the central frequencies of BF1 and BF2 respectively. The scheme propose the situation evolution after the polarization controller (Pol. Cont.) and the photodetector (PD). Reproduced from [25].

- **FREQUENCY-DIVERSITY TECHNIQUE**
  Fundamental: using a frequency-diversity receiver (i.e. a receiver that uses two different frequency channels) allows the removal of the signal spectrum without affecting the beat noise spectrum if the optical signal has a symmetrical spectrum and the two band-pass filters are aligned at the same distance from the center of the signal spectrum, as shown in Fig.21.

  This technique, presented in [45], consists in filtering out the upper and the lower sidebands of an optical signal by means of two band-pass filter (BPFs). The outputs' waveform of the two filters will be highly correlated, while the ASE noises from the two BPFs will not be correlated with each other. Thus, using a balanced receiver, it is possible to cancel out the signal spectrum without affecting the beat noises spectrum. Since this technique does not use polarization properties, it is free from any polarization effects such as PMD and nonlinear birefringence.

  Limitations: if the optical signal experiences CD, its upper and lower sidebands will have different amounts of phase delay resulting in high-frequency components' regeneration. Thus, noise measurements at low frequencies are preferable. Another limit of this technique is the difficulty of using it with non-symmetrical optical spectrum's signals [25].

- **SYNCHRONOUSLY GATED SIGNAL TECHNIQUE**
  Fundamental: this approach, presented in [46], can be applied to any optical signal carrying synchronous traffic with a repetitive header structure, such as SONET/SDH frames.

  By means of a gating device (i.e. an intensity modulator) only the repetitive patterns of each header are allowed to pass, while all the other parts of the frames, payload data included, are suppressed. Thus, the discrete tones of the repetitive patterns in the frequency domains are distinguishable regardless of the payload pattern length, revealing the noise spectrum for monitoring the OSNR, as showed in Fig.22.
  Since this technique does not utilize polarization properties, it is free from any polarization effects such as PMD and nonlinear birefringence. Its schematic diagram is depicted in Fig.23.

  Limitations: if the OSNR needs to be monitored at a transparent optical node where there is no optical-electrical-optical (OEO) conversion, the gating signal acquisition could be difficult. In addition, this technique requires a large amount of optical power.

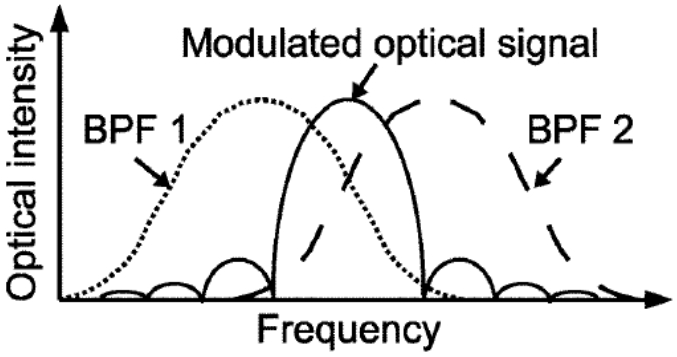

Fig. 21 Filtering of the lower and upper sidebands of an optical signal. Reproduced from [45]**.**

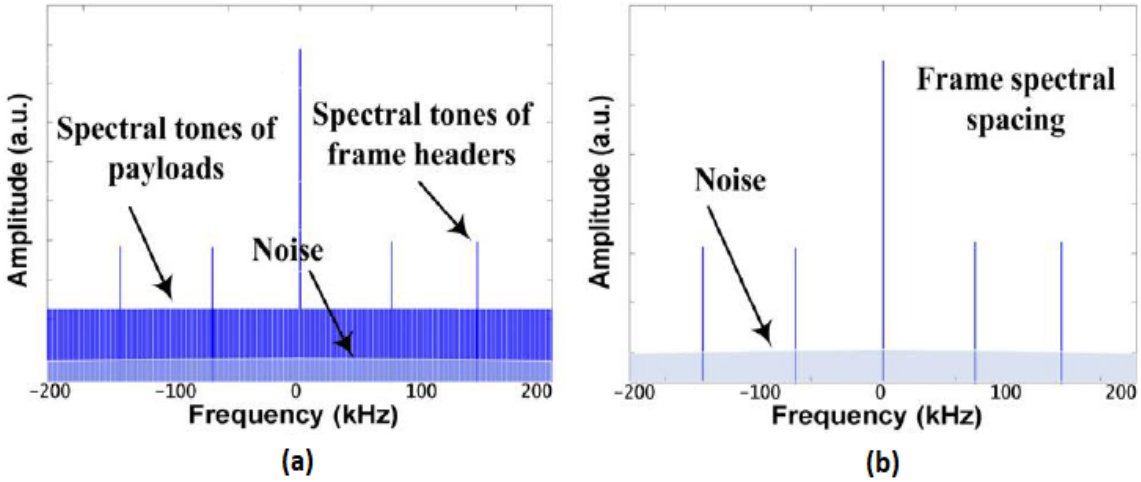

Fig. 22 RF spectrum of the synchronous traffic with (a) and without (b) the gated headers. Reproduced from [46]**.**

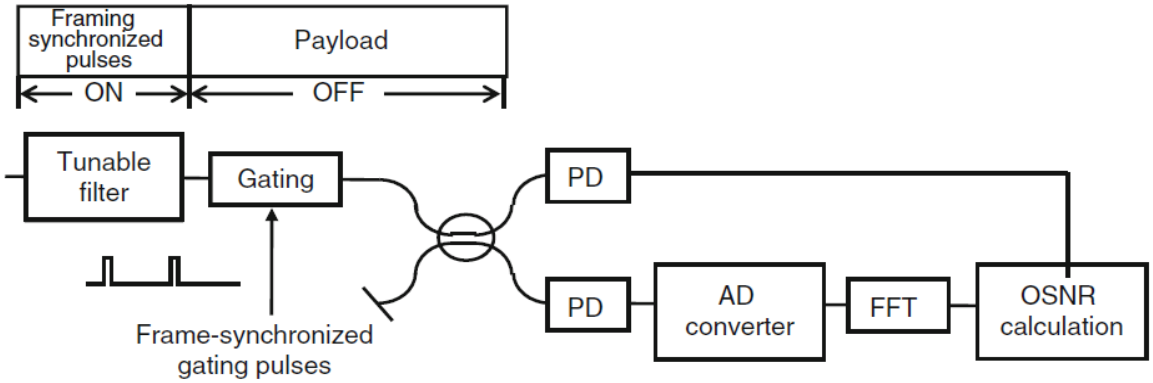

Fig. 23 Schematic diagram of the synchronously gated based monitoring technique. Reproduced from [25]**.**

3.5 OPTICAL AMPLIFIERS OPERATING CONDITION BASED TECHNIQUE

Fundamental: this technique, proposed in [47], bases its OSNR estimations on the characteristics of the erbium-doped fiber amplifiers (EDFAs) instead of measuring the OSNR directly from the optical signal.

The OSNR at EDFA's input can be considered infinite, while at its output it will be equal to [47]:

$$OSNR_{EDFA}\,[dB] = P_{in}\,[dBm] + OSNR_0$$

where:

- P_{in} represents the signal power at the EDFA input
- $OSNR_0$ represents a constant related to the noise characteristics of the EDFA (usually has a wavelength-dependent value)

$OSNR_0$ can be measured while P_{in} can be obtained monitoring the input of the EDFA. Therefore, for WDM signals, the channel power monitoring at the input of every EDFA allows the estimation of the OSNRs of all the channels simultaneously. In case the optical link is constituted by multiple EDFA spans, the OSNRs of the WDM signals at the output of the link is [47]:

$$OSNR_{link}(\lambda) = 1\Big/\sum_{i=1}^{N}\left(1/OSNR_{EDFA,i}(\lambda)\right)$$

where:

- λ represents the channel wavelength
- N represents the number of EDFAs comprising the optical link

Limitation: the estimation of $OSNR_{link}(\lambda)$ requires the optical power of each channel to be monitored at the input of every EDFA, considerably increasing the costs.

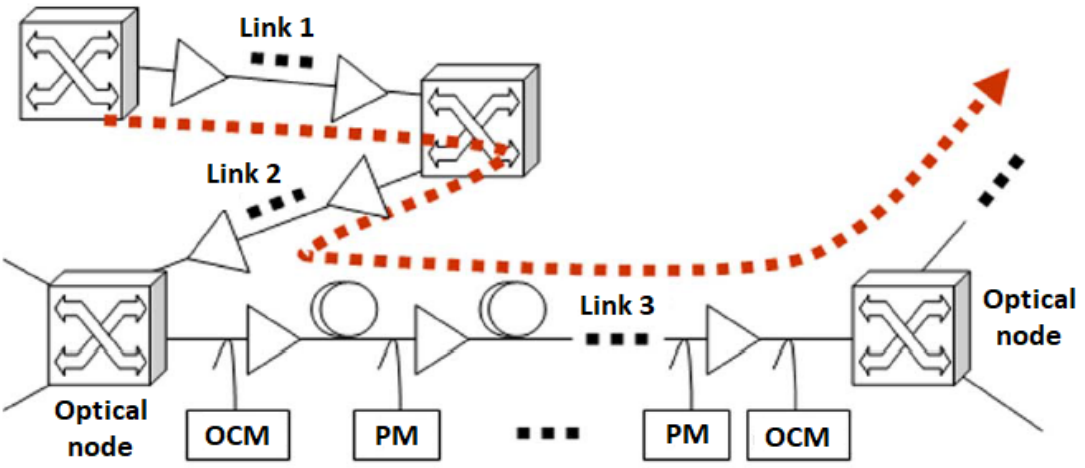

Fig. 24 Schematic diagram of the optical amplifiers operating conditions-based technique. OCM: Optical Channel Monitor, PM: Power Monitor. Reproduced from [47]**.**

3.5.1 LINK-BASED TECHNIQUE

Assumption: with this technique the points of the channel where the power is monitored are restricted to only the input and the output of the link, as shown in Fig.24. This monitoring is made by means of optical channel monitors (OCMs) [47].

The optical signal OSNR is calculated thanks to the channel powers measured at every EDFA through which the signal passes: the OPM gets periodic updates from OCMs and EDFAs with the power information through the management channel, as shown in Fig.25. Thanks to these information it is able to calculate the $OSNR_{link}(\lambda)$ of each channel wavelength and send it to the OPM manager which will update a database. Finally, an end-to-end OSNR estimation is made [48]. This technique is insensitive to CD and any polarization effects.

3.5.2 LINK-BASED TECHNIQUE POTENTIAL PROBLEMS

With this approach, OSNR monitoring could be limited by failures of the management channel or by the presence of few power monitors. In addition, its accuracy is limited by two main factors:

- TOTAL POWER MONITORING: if the number of wavelength channels is very small, the channels power could be overestimated due to the accumulated broadband optical noise. Indeed, monitoring error increases as the number of wavelength channels decreases (because the sum of channels powers becomes comparable to the optical noise's power) and as number of spans per link increases (because the optical noise is invariably accumulated). Anyway, using monitored sets of $OSNR_{EDFA}$ within the link, allows the possibility of calibrating out the noise power from the total power [47].

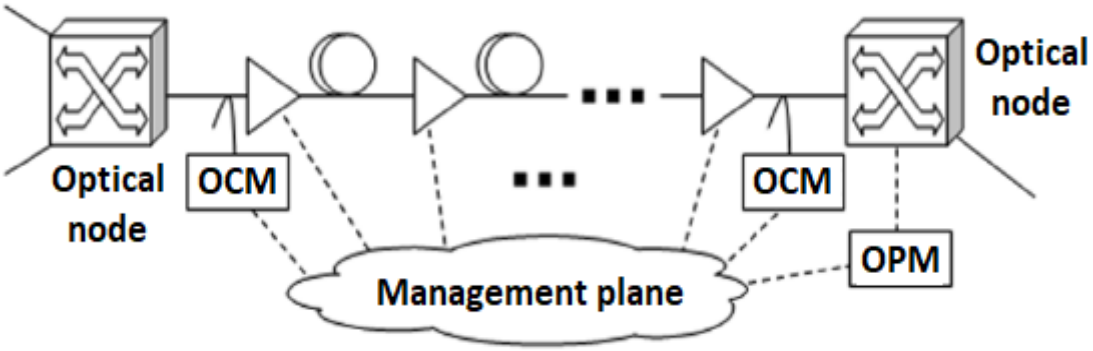

Fig. 25 Schematic diagram of the $OSNR_{link}(\lambda)$ monitoring. OPM: Optical Performance Monitoring. Reproduced from [48].

- GAIN-TILT VARIATION OF EDFAs: Variation of the gain-tilt among EDFAs could create errors in the OSNR estimation, because the technique assumes all the EDFAs within a link with the same gain-tilt: as the number of EDFAs or gain-tilt variation increase, the monitoring error increases as well. Anyway, the problem can be solved adding one or two OCMs at the intermediate EDFAs [47].

3.6 ASYNCHRONOUS AMPLITUDE HISTOGRAMS (AAH) TECHNIQUE

Assumption: this technique takes advantage of the fact that the degradation of a digital optical signal caused by noise, crosstalk and dispersion can be detected evaluating amplitude histograms [49][50].

An amplitude histogram is generated detecting an optical signal by means of a photodiode with high bandwidth and then sampling the electrical signal asynchronously (i.e. without the need for clock recovery) at an arbitrary rate much lower than the symbol rate. A sufficient number of samples, taken at arbitrary time slots, is required for the performance of this technique to be considered reliable. Furthermore, the gate time of the sampling unit (i.e. the pre-set period after which the value of the counter is reset to zero) should be a small fraction of the bit duration to avoid loss of information due to averaging effects (for data-rates of Gb/s, a gate time in the range of few ps is suitable) [49]. These features potentially reduce the cost of the monitor technique allowing its application to signals with arbitrary bit rates. Besides that, the analysis of asynchronous histograms can be performed using relatively simple algorithms, which may be implemented via software [50].

As showed in Fig.26, an AAH typically shows two peaks: one around the electrical current value related to the "0 bit" and one around the electrical current value related to the "1 bit", respectively denominated "space" and "mark". However, it is not possible to en-

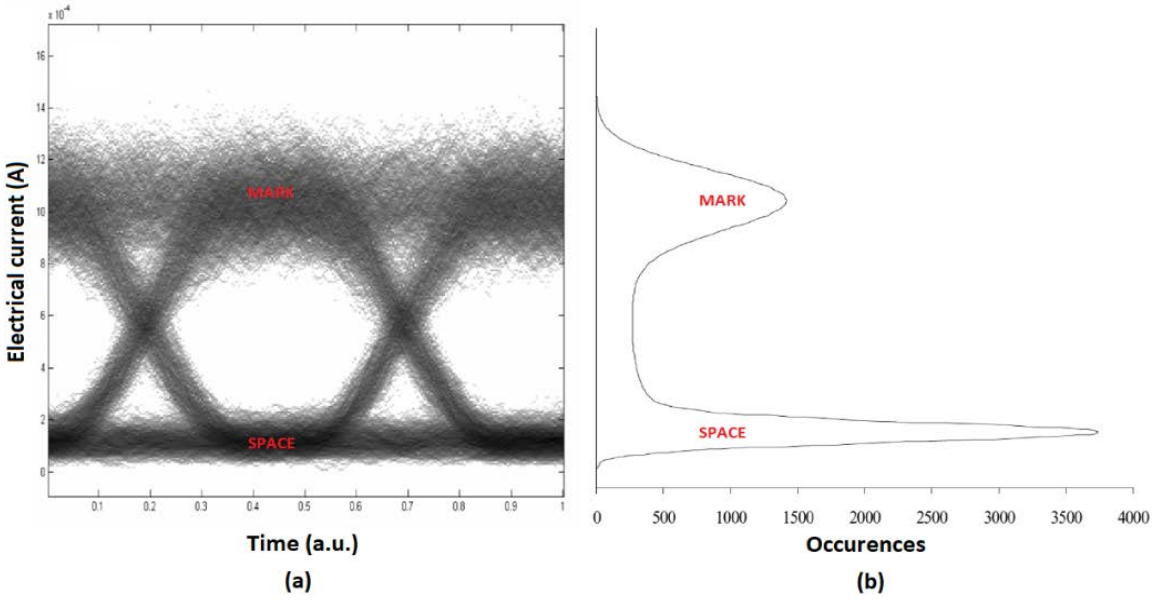

Fig. 26 Example of an eye pattern (a) and the corresponding asynchronous histogram (b). Reproduced from [51]**.**

tirely dissociate the samples corresponding to the mark and space symbols due to a large number of samples located between the two peaks acquired during the transition between the two symbols, also named as "crosspoint data". Optical impairments as ASE noise, crosstalk or fiber dispersion (i.e. group velocity dispersion) can be directly correlated to variations in the shape of AAHs, as was first presented by Hanik *et al*. in [49]. Indeed, amplifier noise broadens and reduces the magnitude of the two peaks, crosstalk gives birth to a floor effect around the mark peak, while fiber dispersion acts both on the slopes (i.e. the distance between the peaks) and the amplitudes of the two peaks, also significantly increasing the crosspoint data amplitude. All these effects are visible in Fig.27.

AAHs may be acquired by sampling the optical signal at an arbitrary rate in the electrical [52] or optical domain [53]. In the former case, the signal is detected using a fast photodetector and electrically sampled at an arbitrary bit rate using an unsynchronized oscilloscope. On the other hand, in the optical sampling case, the samples are produced by an optical sampling gate followed by a slow photodetector and a sample counter.

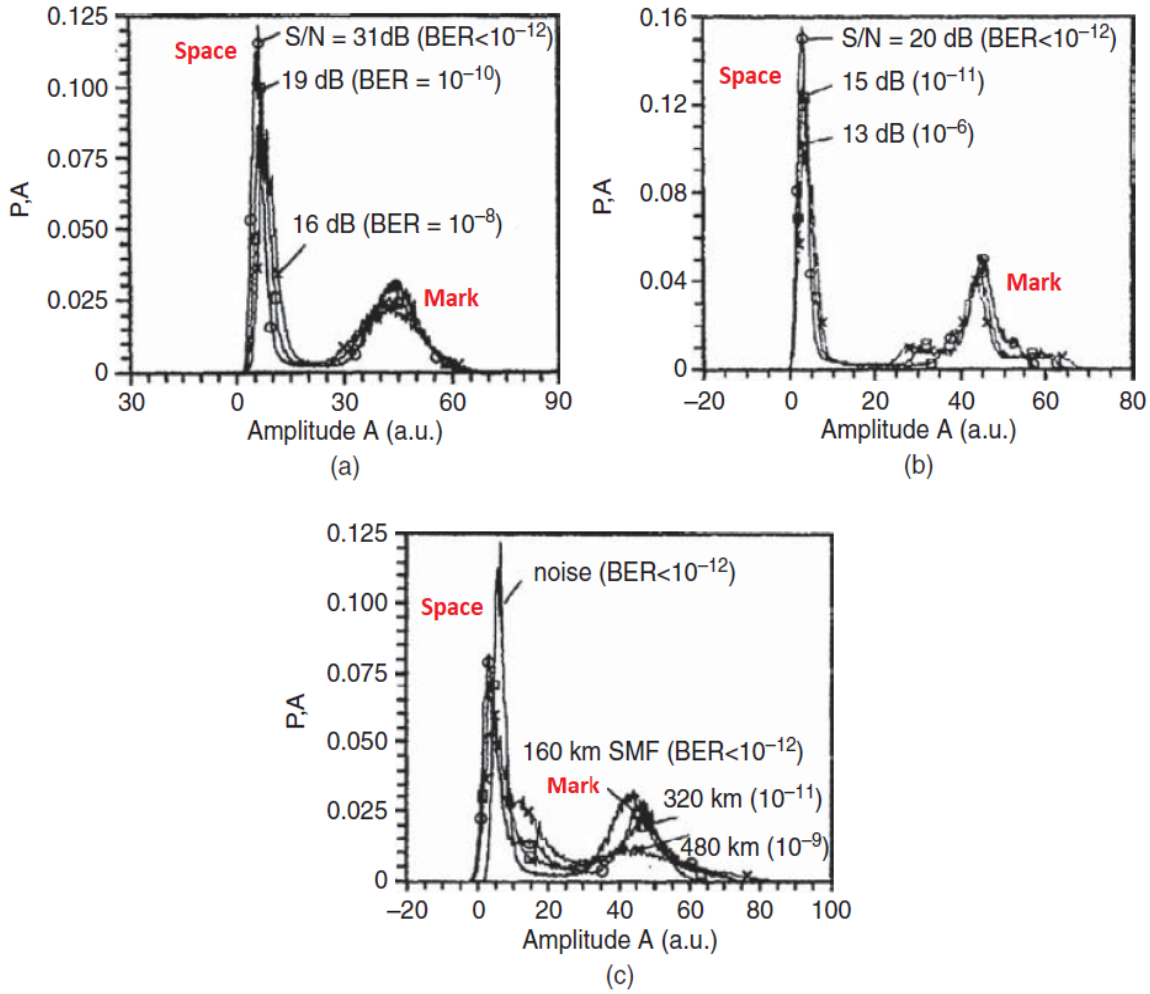

Fig. 27 Effects of optical impairments on the asynchronous histograms shapes: (a) ASE noise effects, (b) intraband crosstalk effects, (c) fiber dispersion effects. Reproduced from [50].

3.6.1 AAH OSNR MONITORING TECHNIQUE

The OSNR of a signal can be estimated analyzing its AAH, as proposed in [51]: namely comparing the measured asynchronous histogram (MAH) acquired from the signal under analysis, with a reference asynchronous histogram (RAH) obtained from the same signal during a calibration stage; these comparison process is depicted in Fig.28.

As shown in [51], this method relies on including the impact of the additional ASE noise on the RAH to match the MAH, or vice-versa. Then, by determining the amount of ASE noise needed to achieve the match, the OSNR penalty between the signal under analysis and the reference signal can be estimated. Furthermore, since the AAH monitoring technique relies on the evaluation of ASE noise impact on the shape of the AAH independently of the signal waveform, it becomes possible the usage of simple optical processing techniques to enhance the accuracy of the OSNR estimation.

A possible limitation of this technique is related to the fact that the maximum measurable OSNR decreases with the power at the input of the optical monitoring system and with the variance of the noise generated in the OMS. However, this limitation can be overcome by lowering the value of the reference OSNR.

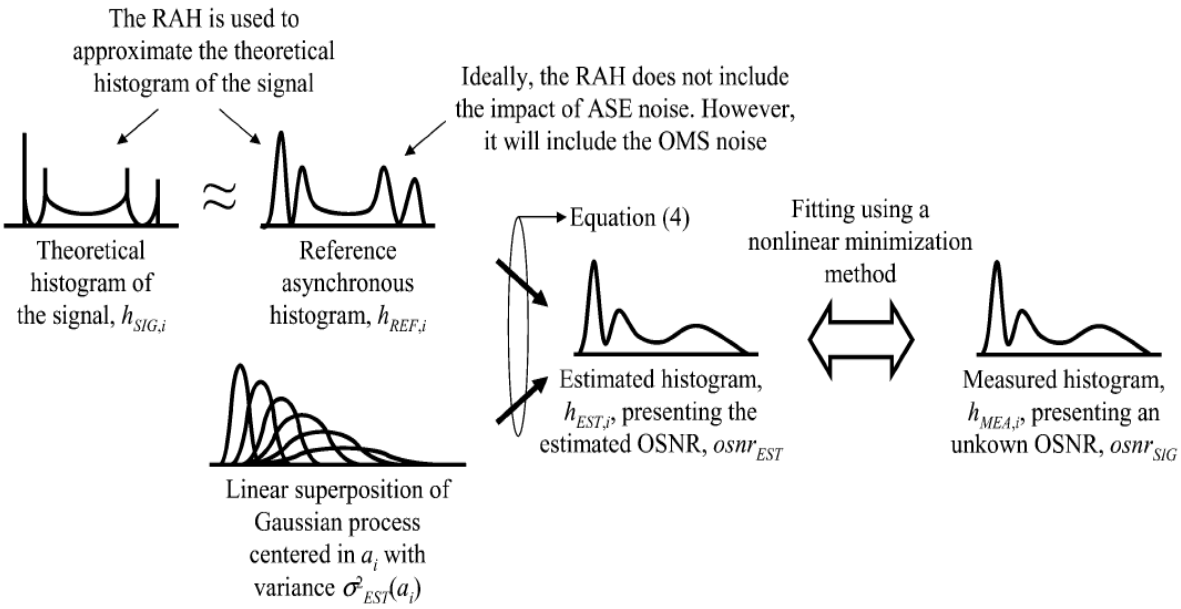

Fig. 28 Schematic diagram of the comparison process between the histograms. Reproduced from [51]**.**

3.7 OSNR MONITORING TECHNIQUES FOR DIGITAL COHERENT DETECTION SYSTEMS

The advances in coherent detection and DSP over the past years, have brought to the rise of a new OSNR monitoring approach, in which the monitoring information are provided

directly by the DSP as a by-product of the digital coherent receiver [54].
Coherent detection systems have simplified the demultiplexing process of polarization multiplexed (PM) signals, allowing PM to be widely used in almost all the DSP based coherent transmission systems [55]. Thereby, PB/polarization diversity in-band OSNR monitoring techniques (see subsection 3.2) are no longer suitable for this kind of scenario. In addition, the employment of Nyquist WDM with very tight WDM channel spacing has increased [55], making LI based out-band OSNR monitoring techniques (see subsection 3.1) impractical. Therefore, the techniques proposed in the previous subsections, which refer to systems where direct detection is employed, need to be complemented with new OSNR monitoring techniques for digital coherent systems. In Fig.29, a standard coherent receiver with DSP algorithm blocks, is reported.

The OSNR monitoring technique presented in [56], exploits the higher-order statistical moments of the equalized signal from an adaptive filter in coherent optical receivers (i.e. immediately after the "Adaptive Equalization" block in Fig.29). Since the variations of the equalized signal envelope can be considered to be mainly caused by the ASE noise (linear distortions such as CD and PMD, ideally, should be fully compensated by the adaptive filter), and that fiber nonlinear effects can be neglected (assuming a low launched power), the OSNR can be calculated as [56]:

$$OSNR_{dB} = 10log_{10}(CNR) + 10log_{10}\left(\frac{R_s}{B_{ref}}\right)$$

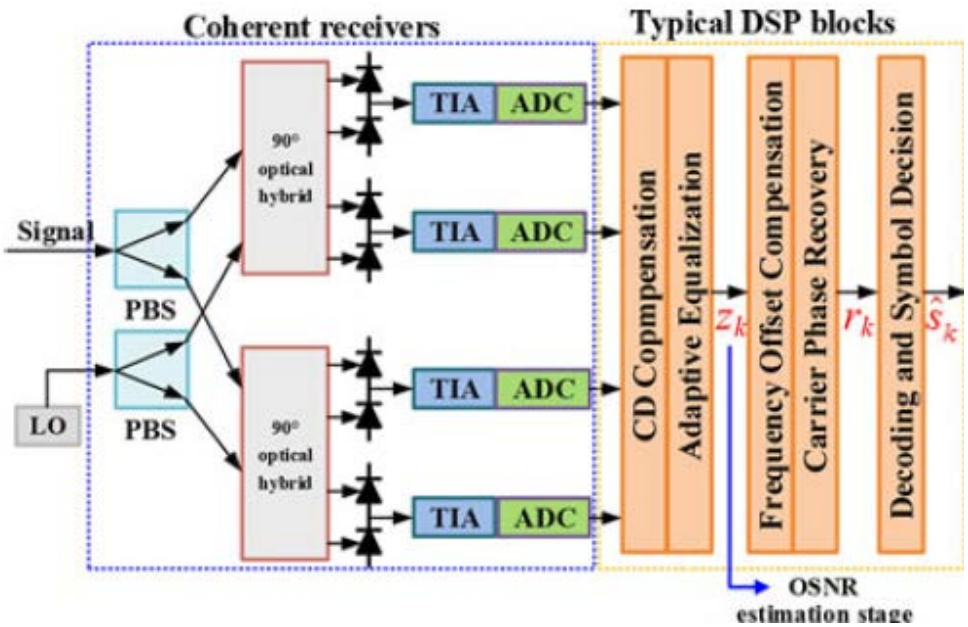

Fig. 29 Coherent optical receiver with DSP blocks. Reproduced from [54].

where:
- R_s represents the symbol rate
- B_{ref} represents the reference bandwidth

- R_s/B_{ref} represents a scaling factor to adjust the measured noise power bound by the adaptive filter bandwidth
- CNR represents the carrier-to-noise ratio [56]:

$$CNR = \frac{\sqrt{2\mu_2^2 - \mu_4}}{\mu_2 - \sqrt{2\mu_2^2 - \mu_4}}$$

where:
- μ_2 represents the second moment order of the output signal from adaptive filter
- μ_4 represents the fourth moment order of the output signal from adaptive filter

The proposed technique operates phase insensitively and uses "blind" non-data-aided channel acquisition (i.e. the received data are unknown) by gradient algorithms, like constant-modulus algorithm (CMA). On the other hand, a data-aided channel acquisition scheme (i.e. where the actually sent data are known) relying on training sequences (TS) can be used, as for example, in [57]. The main difference between the two approaches are that the data-aided acquisition has a higher estimation accuracy and is faster, while the "blind" approach has a higher bandwidth efficiency.

Another way to estimate the OSNR has been proposed in [58], where the authors used the error vector magnitude (EVM) of fully equalized signals as an OSNR estimator. The EVM describes the effective distance of the received complex symbol from its ideal position in the constellation diagram, as showed in Fig.30, in which the red cross represents the actually received value, while the black dot represents the ideal transmitted value. The technique assumes that the received optical field is perturbed only by AWGN. The EVM is defined as [58]:

$$EVM = \frac{\sigma_{err}}{|E_{t,m}|}, \qquad \sigma_{err}^2 = \frac{1}{I}\sum_{i=1}^{I}|E_{err,i}|^2, \qquad E_{err,i} = E_{r,i} - E_{t,i}$$

where:
- E_{err} represents the error vector
- σ_{err} represents the root mean square of E_{err}
- $|E_{t,m}|$ represents the magnitude of the power of the longest constellation vector
- I represents the number of the transmitted data
- E_r represents the actually received signal vector
- E_t represents the ideal transmitted vector

The OSNR can be finally estimated by means of an EVM-based approach as [59]:

$$OSNR_{estimated} = \frac{P_{in}}{P_{ASE}} = \frac{E(|E_t|^2)}{E(|E_r|^2)}$$

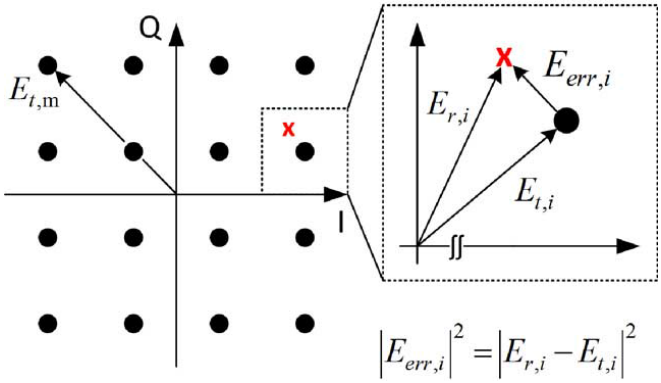

Fig. 30 Ideal constellation diagram for a 16-QAM with an actually transmitted value (red cross) that deviates from the ideal one (black dot) of an error represented as the vector E_{err}. Reproduced from [58]**.**

where:

- P_{in} represents the signal power
- P_{ASE} represents the ASE noise power
- $E(\cdot)$ represents the expectation value

In long-haul transmission systems, the abovementioned techniques will considerably under-estimate the OSNR, because in a dispersion uncompensated scenario, nonlinear distortions are typically treated as noise and are indistinguishable from amplifiers ASE noise. Indeed, a realistic long-haul transmission system operates in the weakly nonlinear regime. Thus, new techniques able to monitor the OSNR in a nonlinear insensitive way have been studied. For example, in [59], Dong *et al*. propose a method that leverages the amplitude noise correlation across neighbouring symbols for the intra-channel nonlinearities characterization. Fiber nonlinear distortions are shown to depend only on the power of the launched signal, but not on OSNR, therefore isolating them from the ASE noise. Problems with this approach arise considering WDM systems, where inter-channel nonlinearities occur [54]. Therefore, some other way to characterize inter-channel nonlinearities have been proposed: in [60], for example, the authors used the amplitude correlation functions between two polarizations as well as the neighbouring symbols to remove the contribution of the nonlinearity-induced signal distortions.

The OSNR monitoring techniques listed in this subsection so far, rely on full speed coherent receivers and thus are not optimal to be used for distribute monitoring at the intermediate nodes of the network. Indeed, at the intermediate nodes, the cost of OSNR monitoring has to be low and should be based on low-speed hardware solutions. In [61], Do *et al.* presented a data-aided DSP-based technique, that uses low-bandwidth coherent receivers and sub-Nyquist sampling speed. By means of this method, the authors, have been able to estimate a wide range of OSNRs with accuracy within 1 dB for up to 1000-km transmission distance.

4 DISAGGREGATED NETWORKS

Convergence, i.e. taking functions that once resided in separate devices and combining them in a single system, has always been a trend for telecommunication operators [62]: this approach allowed saving on Capex (e.g. fewer boxes) and Opex (e.g. simplified management of the network and its elements).

As pointed out in [62], the key element to the success of the integration/aggregation approach has been the presence of a unified element management system (EMS)/network management system (NMS), which could manage the whole network elements. Historically, the downside of the aggregation strategy has always been the fact that the unified EMS/NMS has been built by the equipment supplier itself.

Nowadays, also thanks to the rise of the software-defined networking (SDN) and network functions virtualization (NFV), the telecom industry is moving towards a more dynamic and flexible approach: the networks disaggregation [63]. Disaggregation in networks is the result of the application of certain technologies as virtualization, use of x86-based commodity hardware, software-based automation, use of open source and separation of control planes from forwarding planes by the network operators. In [62], supporting the disaggregated networks vision, some examples of changes in the operators' strategies are listed.

Disaggregation is the inverse approach of what has occurred during the past years: decoupling the components of integrated systems from each other. This paradigm implies a functional disaggregation rather than block-by-block disaggregation [64] and allows the users to select the mix of hardware and software that best meets their needs. The disaggregated networks approach involves an evolution from chassis-based (proprietary) network elements to commodity (off-the-shelf) components, the so-called *white boxes*, where generic off-the-shelf hardware can be purchased from any vendor and customized with software from different sources. This paradigm will allow telecom operators to size their infrastructure as needed [65].

As described by Riccardi *et al*. in [66], the white box model is the evolution of the bare metal operational model. While in the second the operators source their hardware supplies directly from the original design manufacturers (ODMs) and adapt free and open source software to it, in the white-box approach ODMs provide to the operators devices where some pre-installed operating system is present together with some level of support. On the other hand, with the so-called *black box* approach, the single vendor closely aggregates both the hardware and software and assumes oversight of hardware components. Finally, in the middle between white and black box approaches there is *brite box* operational model (i.e. branded white box HW), where, as in white boxes, the operating system and application software are disaggregated from the hardware. Brite boxes have pre-installed third-party operating system and come provisioned for a tailored level of lifecycle support from the vendor. All the above mentioned approaches are represented in Fig.31 together with the graded support spectrum that an operator has to sustain during their lifetime cycle.

White boxes are therefore a key element for providing the required disaggregation between software and hardware, including the separation between control, management and

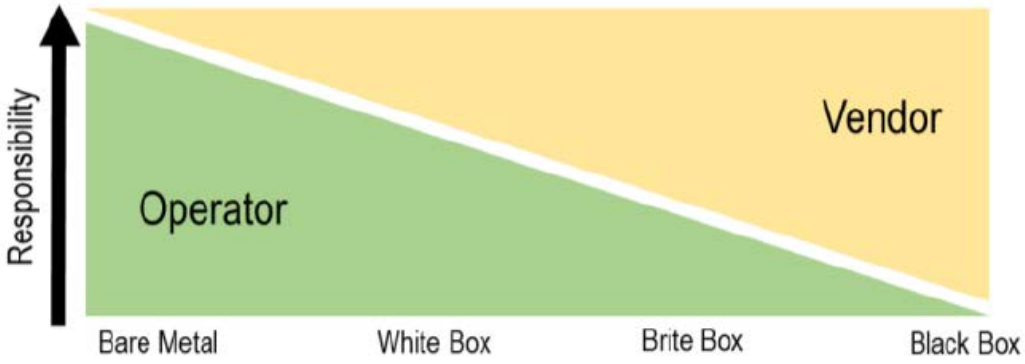

Fig. 31 Representation of the four different operational models with the responsibility level spectrum of each one split between operator and vendors. Reproduced from [66].

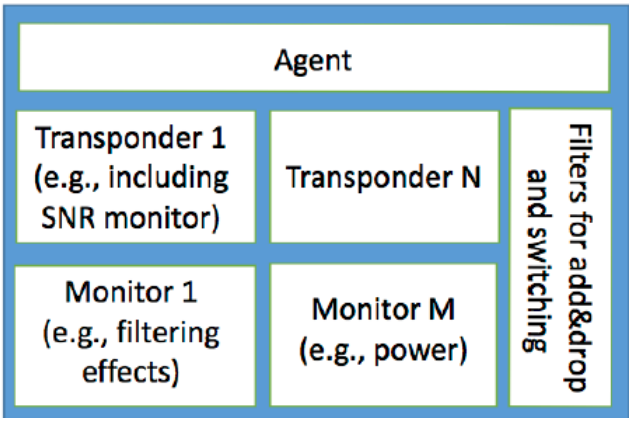

Fig. 32 Example of white box architecture. Reproduced from [67].

forwarding planes. An example of a generic white box architecture is shown in Fig.32: its hardware is assembled with modules provided by different vendors that should interoperate each other, while an agent interfaces with the software-based control and management plane.

In [66] the authors, who considered a metro/regional WDM transport system (WDM-Sys), have identified four possible optical disaggregation models to replace the established aggregated paradigm based on single vendor systems. Each one of them implies a different level of involvement of the Telecom operator in the process of design, assembly and integration of the WDM system.
The metro/regional WDM-Sys is composed by optical network elements (ONEs), which are pieces of equipment housing homogeneous network functions, and are classified as [66]:

- Client to WDM adapter, TP: this category includes Transponders (i.e. 1-1 mapping of clients to line side interfaces), Muxponders (N-1 mapping and multiplexing), switchponders (N-M mapping, switching and multiplexing).

- Multi-degree Reconfigurable Optical Add-Drop Multiplexer, M-ROADM: it includes Add&Drop, switching, amplification and equalization optical functions.
- Line Terminal, LT: single line side optical multiplexer fitted with colourless functionalities.
- In Line Amplifier, ILA: amplifiers inserted between LTs or M-ROADMs to balance optical attenuation.

The management and control systems see the ONEs as a single management entity through a suitable open application programming interface (OpenAPI), also named South Bound Interface (SBI). On the other hand, by means of a North Bound Interface (NBI), the management and control planes communicate with higher-level entities (e.g. the SDN controller) enabling enhanced network programmability [66].

Telecommunications operators can be involved in several degrees of depth in the design, assembly, integration and testing of the whole WDM-Sys. Based on this assumption, in [66], the authors listed three different kind of network visions:

- **Fully Aggregated Optical Domains:** the optical system lifecycle management is responsibility of the system vendor that provides both the proprietary WDM transport controller and all the ONEs as foreseen by the pure black box approach. This paradigm is illustrated in Fig.33a.
- **Partial Disaggregation, Open Line System (OLS) and Multi-Vendor Transponders:** this approach enables the disaggregation to the digital to WDM adaptation layer (DtoWDM), i.e. the TPs, which adapt the digital client signals to the analogical media channels. On the contrary, the WDM Analog transport layer (A-WDM), remains a proprietary black box analogue transport system. The open term refers to the fact that the system is open to be used by any signal that follows the behaviour specified by the Single Wavelength Interfaces (SWI). The system depicted in Fig.33b, which describes this approach, shows the presence of an OLS-NBI API needed to configure and report event from the OLS.
- **Full Disaggregation, Multi-Vendor Optical Network Elements:** this approach, represented in Fig. 33c, involves a strong presence of operators in the WDM-Sys lifecycle. Potentially, both the ONEs from the A-WDM and DtoWDM layers are purchased from different vendors and the control intelligence is moved to the WDM controller, which is vendor agnostic.

To support control and management of the white-boxes, standardized data models are required: for example, YANG is a data modelling language that enables interfacing with the control and the management system and is supported by the emerging NETCONF protocol standardized by the IETF [67][68].

The disaggregated networks paradigm could bring lot of benefits to the operators, among which efficient scaling (i.e. an initial low spend for year one deployments with the ability to grow as the traffic increases and more capacity is required) and the ability to share functions across different resources (thus sharing spaces on servers that are already present) and therefore saving costs in Opex [62][69].

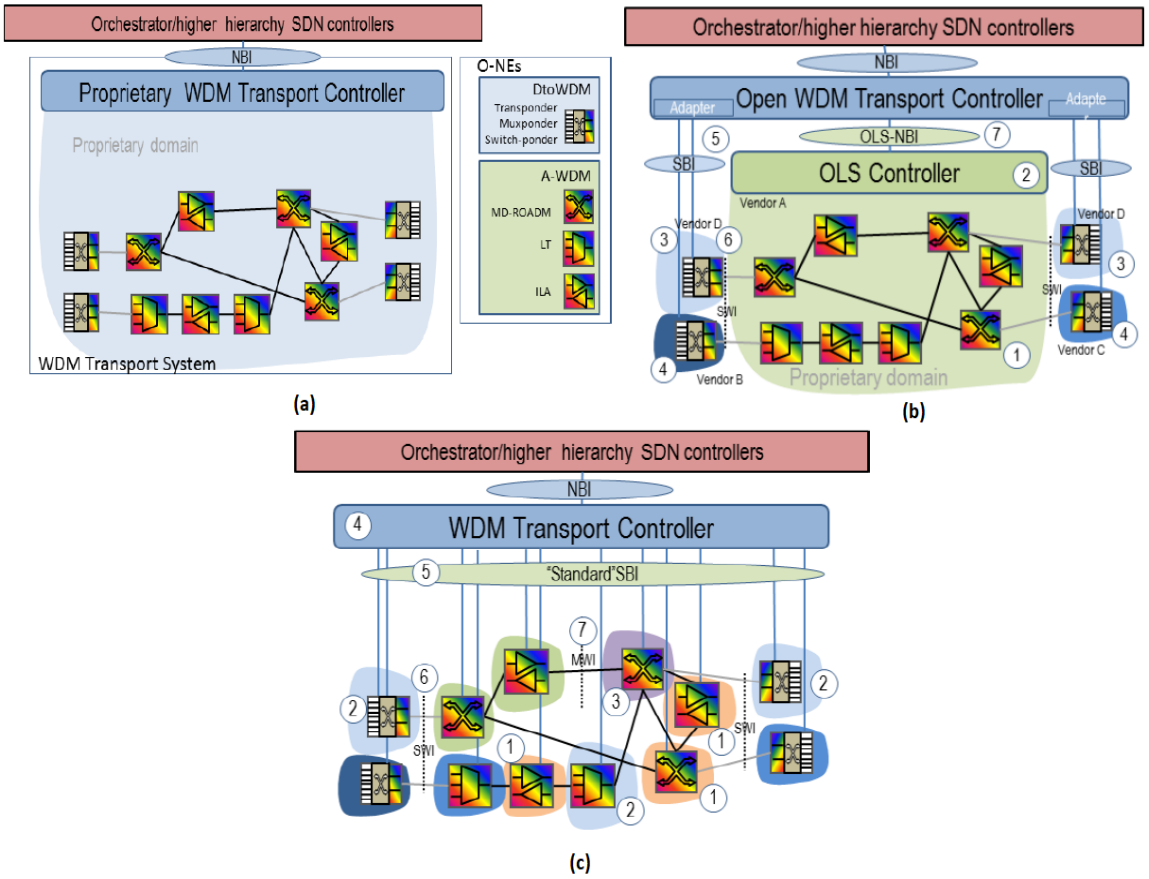

Fig. 33 The three different network approaches: (a) Fully Aggregated WDM Transport System, (b) Partially Disaggregated WDM Transport System and (c) Fully disaggregated WDM Transport System. Reproduced from [66].

Undoubtedly, maintaining the required performance and features without lowering the networks reliability is a key challenge that the operators, who decide to move towards a disaggregated network paradigm would face, along with the integration with legacy network elements and management systems [62]. In addition, proactive and reactive automation of optical disaggregated networks with white box switches could represents another big challenge that needs to be addressed [64]. Such automation is based on processing real-time network monitoring parameter and learning from the effects of the decisions previously taken. Therefore, another fundamental task to accomplish is the development of new optical monitoring techniques able to deliver the feedback needed for guaranteeing the end-to-end QoT and QoS. In this context, the OSNR monitoring techniques described in the previous section represent an important starting point.

5 OBJECTIVES AND EXPECTED RESULTS

The focus of this project is to exploit the flexibility and modularity provided by the disaggregated network paradigm to reduce both Capex and Opex, when automatizing the operations of the network, namely leveraging open source software solutions running on inexpensive commodity hardware. Thus, in this context, the research of novel flexible transmission technologies becomes one of the main objectives of the project: they should be able to add flexibility, programmability and modularity to the network so that the capacity/reach requirements of the next generation networks would be fulfilled.

In addition, as described in the previous sections, an important subsystem of the disaggregated network elements is the optical monitoring technique, that has to deliver the feedback needed to guarantee end-to-end QoT and QoS, helping to close the cognition cycle of the cognitive-based network control. Thus, another main goal of the ONFIRE project is the investigation and development of cost-effective solutions for non-intrusive in-band performance monitoring, providing at the same time the corresponding open programmable network elements (i.e. the white boxes), which allow the continuous adjustment and re-optimization of the network settings. Finally, network's margins reduction could be another efficient way to decrease the operator costs: therefore new techniques to reduce or leverage their impact on the network should be investigated, taking into account that lowering the margins could be more challenging in a disaggregated optical network scenario due to the additional losses induced by the usage of commodity hardware.

The expected results are related to the study and the design of open disaggregated architectures (i.e. white boxes). In particular, suitable transmission schemes will be enhanced based on white boxes approach and flexible paradigm, including system margins reduction, facilitating the interoperability and the adaptation to the network conditions variations. Thus, a relevant objective is to equip the system elements (e.g. multi-flow programmable transceivers) with flexible advanced functionalities, integrating statistical multiplexing and the feedback of monitoring techniques. In addition, the development of new OPM techniques agnostic to the signal waveform will be addressed: low-cost techniques for signal analysis will be pursued together with the development of OSNR monitoring algorithms, including the investigation of the needed parameters, being also extensible for a polarization-resolved complex analysis of the signal (e.g. employing polarization/phase-resolved spectrometry and/or coherent reception). The integration of white-boxes approach with OPM techniques will constitute the basis on which disaggregated network paradigm will be assessed. Certainly, all these improvements will have to interwork with the already deployed network environment, composed by optical black boxes. The proposed data plane architecture will be then integrated with the corresponding control, orchestration and management elements. Finally, the obtained results must be validated by means of simulations and experiments.

6 METHODOLOGY AND PLANNING

6.1 METHODOLOGY

A strict process of research, reading and understanding of the works presented so far in the literature was the starting point on which the ESR1 has based the state of the art presented in this document. In fact, an initial in-depth review of the investigated topics is essential to allow the detection of potential gaps for new technological developments. To do so, a large amount of reference works were found and reviewed by the ESR1: the most widely bibliographic databases used during the drafting of the report were the Institute of Electrical and Electronics Engineers (IEEE) and the Optical Society (OSA) websites. Also some textbooks have been used as important sources of information. A remarkable knowledge of the state of the art is fundamental to benchmark the devised solutions with respect to other approaches proposed in the literature. Indeed, the drafting and understanding of the state of the art is the basis on which the ESR1 founds his doctoral work, and through which he will be able to improve his knowledge about the optical networking background.

After the identification of new promising approaches, the following step will be to design, analyse and implement the conceived solutions. To do so, different simulation environments will be taken into account, as for example MATLAB, Python and VPI. While the first two are well-known numerical analysis tools useful for the development of numerical models and simulating the system under investigation, the latter is a simulation tool that allows the user to design and test almost all kinds of optical elements in the transmission layer, in a relative fast and easy way.

Validation of the obtained results will be finally carried out comparing them with the experimental data collected in the laboratories. Indeed, both the ONFIRE partners (Barcelona's CTTC and Stuttgart's ALUD Nokia Bell Labs) have laboratories equipped with appropriate facilities for the experimental activities. The ESR1 will have access to CTTC's Optical Networks and Systems Laboratory (ONS Lab) and its ADRENALINE testbed (which includes a photonic mesh network with 4 nodes and 5 bidirectional optical links up to 150 km and an experimental platform for optical transmission systems) and to ALUD's extensive lab equipment (e.g. optical fiber test-beds, optical modulators and receivers, etc.).

In addition, throughout the whole project duration, the ESR1 will have to provide periodic delivery of specific documents (namely deliverables), which will report to the project officer on the status of the ONFIRE project and will provide the obtained results.

Finally, one of the key elements of the project will be the collaboration with the other ESR: namely, the data and the control plane elements respectively experimentally assessed by ESR1 and ESR2, will be integrated each other. The whole interworking system will be then experimentally verified and its performance will be evaluated.

6.2 PLANNING

Refer to the tentative Gantt chart attached at the end of the document.

7 REFERENCES

[1] Y. Pointurier, "Design of Low-margin Optical Networks," *Opt. Fiber Commun. Conf.*, vol. 9, no. 1, p. Tu3F.5, 2016.

[2] P. Soumplis, K. Christodoulopoulos, M. Quagliotti, A. Pagano, and E. Varvarigos, "Network Planning with Actual Margins," *J. Light. Technol.*, vol. 35, no. 23, pp. 5105–5120, 2017.

[3] Ciena, "Liquid Spectrum : Transforming Static Optical Networks into Dynamic, Responsive Assets," *White Pap.*, 2017.

[4] Coriant, "Evolving the Awareness of Optical Networks," *White Pap.*, pp. 1–12, 2017.

[5] Y. Nozu, Y. Aoki, K. Komaki, and S. Okano, "'Conscious optical network' with reliability and flexibility," *Fujitsu Sci. Tech. J.*, vol. 52, no. 2, pp. 75–82, 2016.

[6] J.-L. Auge, "Can we use Flexible Transponders to Reduce Margins?," *Opt. Fiber Commun. Conf. Fiber Opt. Eng. Conf. 2013*, p. OTu2A.1, 2013.

[7] J. Pesic, T. Zami, P. Ramantanis, and S. Bigo, "Faster return of investment in WDM networks when elastic transponders dynamically fit ageing of link margins," *Opt. Fiber Commun. Conf. 2016*, no. 1, pp. 8–10, 2016.

[8] J. Pesic and A. Morea, "Operating a Network Close to the " Zero Margin " Regime Thanks to Elastic Devices," p. 2015, 2015.

[9] Ciena, "Transforming Margin into Capacity with Liquid Spectrum," 2005.

[10] T. Fehenberger, A. Alvarado, P. Bayvel, and N. Hanik, "On Achievable Rates for Long-Haul Fiber-Optic Communications," vol. 23, 2015.

[11] C. Diniz *et al.*, "Network Cost Savings Enabled by Probabilistic Shaping in DP-16QAM 200-Gb/s Systems," *Opt. Fiber Commun. Conf.*, vol. 1, 2016.

[12] F. Buchali, F. Steiner, G. Böcherer, L. Schmalen, P. Schulte, and W. Idler, "Rate Adaptation and Reach Increase by Probabilistically Shaped 64-QAM: An Experimental Demonstration," *J. Light. Technol.*, vol. 34, no. 7, pp. 1599–1609, 2016.

[13] A. Barbieri, D. Fertonani, and G. Colavolpe, "Time-frequency packing for linear modulations: Spectral efficiency and practical detection schemes," *IEEE Trans. Commun.*, vol. 57, no. 10, pp. 2951–2959, 2009.

[14] T. Zami, A. Morea, F. Leplingard, and N. Brogard, "The relevant impact of the physical parameters uncertainties when dimensioning an optical core transparent network," *Eur. Conf. Opt. Commun. ECOC*, no. January, pp. 19–21, 2008.

[15] E. Seve, J. Pesic, C. Delezoide, and Y. Pointurier, "Learning process for reducing uncertainties on network parameters and design margins," *Opt. Fiber Commun. Conf.*, vol. 10, no. 2, p. W4F.6, 2017.

[16] I. Sartzetakis, K. Christodoulopoulos, C. P. Tsekrekos, D. Syvridis, and E. Varvarigos, "Estimating QoT of Unestablished Lightpaths," *Opt. Fiber Commun. Conf. 2016*, pp. 3–5, 2016.

[17] A. Mitra, A. Lord, S. Kar, and P. Wright, "Effect of link margin and frequency granularity on the performance of a flexgrid optical network.," *Opt. Express*, vol. 22, no. 1, pp. 41–6, 2014.

[18] L. D. Notivol, S. Spadaro, J. Perelló, and G. Junyent, "Cognitive science applied to reduce network operation margins," *Photonic Netw. Commun.*, vol. 34, no. 3, pp. 432–444, 2017.

[19] C. Delezoide, K. Christodoulopoulos, A. Kretsis, N. Argyris, G. Kanakis, and A. Sgambelluri, "Field Trial of Marginless Operations of An Optical Network Facing Ageing and Performance Fluctuations," *Eur. Conf. Opt. Commun. ECOC*, vol. 4, no. 1, pp. 5–7, 2018.

[20] H. B. Chenoweth, "Soft failures and reliability," *Annu. Proc. Reliab. Maintainab. Symp.*, vol. 6, pp. 419–424, 1990.

[21] K. Christodoulopoulos *et al.*, "Observe-Decide-Act : Experimental Demonstration of a Self-Healing Network," *Opt. Fiber Commun. Conf. Expo.*, pp. 7–9, 2018.

[22] N. Sambo, F. Cugini, A. Sgambelluri, and P. Castoldi, "Monitoring Plane Architecture and OAM Handler," *J. Light. Technol.*, vol. 34, no. 8, pp. 1939–1945, 2016.

[23] A. P. Vela *et al.*, "Soft Failure Localization During Commissioning Testing and Lightpath Operation," *J. Opt. Commun. Netw.*, vol. 10, no. 1, p. A27, 2018.

[24] B. Chomycz, *Planning Fibre Optic Networks*. 2009.

[25] J. H. Lee and Y. C. Chung, "Optical signal-to-noise ratio monitoring," in *Optical performance monitoring*, C. C. K. Chan, Ed. Elsevier, 2010, pp. 21–66.

[26] J. H. Lee, H. Y. Choi, S. K. Shin, and Y. C. Chung, "A review of the polarization-nulling technique for monitoring optical-signal-to-noise ratio in dynamic WDM networks," *J. Light. Technol.*, vol. 24, no. 11, pp. 4162–4171, 2006.

[27] Agrawal, *Nonlinear Fiber Optics*. 2007.

[28] M. Petersson, H. Sunnerud, M. Karlsson, and B.-E. Olsson, "Performance Monitoring in Optical Networks Using Stokes Parameters," *IEEE Photonics Technol. Lett.*, vol. 16, no. 2, pp. 686–688, 2004.

[29] J. P. Gordon and H. Kogelnik, "PMD fundamentals: polarization mode dispersion in optical fibers.," *Proc. Natl. Acad. Sci. U. S. A.*, vol. 97, no. 9, pp. 4541–4550, 2000.

[30] J. H. Lee, D. K. Jung, C. H. Kim, and Y. C. Chung, "OSNR monitoring technique using polarization-nulling method," *IEEE Photonics Technol. Lett.*, vol. 13, no. 1, pp. 88–90, 2001.

[31] J. H. Lee and Y. C. Chung, “Effect of polarization-dependent loss on optical signal-to-noise ratio monitoring technique based on polarization-nulling method,” *Opt. Express*, vol. 14, no. 12, pp. 5045–5049, 2006.

[32] J. Wuttke, P. M. Krummrich, and J. Rösch, “Polarization oscillations in aerial fiber caused by wind and power-line current,” *IEEE Photonics Technol. Lett.*, vol. 15, no. 6, pp. 882–884, 2003.

[33] C. H. Kim *et al.*, “Performance of an OSNR monitor based on the polarization-nulling technique,” vol. 3, no. 6, pp. 388–395, 2004.

[34] J. Lee and Y. Chung, “Improved OSNR monitoring technique based on polarization-nulling method,” *Electron. Lett.*, vol. 37, no. 15, pp. 972–973, 2001.

[35] M. H. Cheung, L. K. Chen, and C. K. Chan, “PMD-insensitive OSNR monitoring based on polarization-nulling with off-center narrow-band filtering,” *IEEE Photonics Technol. Lett.*, vol. 16, no. 11, pp. 2562–2564, 2004.

[36] H. Y. Choi, “Improved Polarization-Nulling Technique for Monitoring OSNR in WDM Network,” pp. 7–8, 2006.

[37] M. Skold, B. Ohson, H. Sunnerud, and M. Karlsson, “PMD-insensitive DOP-based OSNR,” no. X, pp. 3–5, 2005.

[38] Zhenning Tao, Zhangyuan Chen, Libin Fu, Deming Wu, and Anshi Xu, “A novel method to monitor OSNR using a Mach-Zehnder interferometer,” *Tech. Dig. CLEO/Pacific Rim 2001. 4th Pacific Rim Conf. Lasers Electro-Optics (Cat. No.01TH8557)*, vol. 2, p. II-564-II-565.

[39] X. Liu, Y. H. Kao, S. Chandrasekhar, I. Kang, S. Cabot, and L. L. Buhl, “OSNR monitoring method for OOK and DPSK based on optical delay interferometer,” *IEEE Photonics Technol. Lett.*, vol. 19, no. 15, pp. 1172–1174, 2007.

[40] S. K. Shin, K. J. Park, and Y. C. Chung, “A novel optical signal-to-noise ratio monitoring technique for WDM networks,” *Opt. Fiber Commun. Conf. Tech. Dig. Postconf. Ed. Trends Opt. Photonics Vol.37 (IEEE Cat. No. 00CH37079)*, vol. 2, pp. 182–184.

[41] C. J. Youn, S.-K. Shin, K.-J. Park, and Y. C. Chung, “OSNR monitoring technique based on high-frequency receiver noise,” no. November, pp. 34–38, 2001.

[42] T. B. Anderson, K. Clarke, S. D. Dods, and M. Bakaul, “Robust, Low Cost, In-Band Optical Signal to Noise Monitoring Using Polarization Diversity,” *OFC/NFOEC 2007 - 2007 Conf. Opt. Fiber Commun. Natl. Fiber Opt. Eng. Conf.*, pp. 1–3, 2007.

[43] C. J. Youn, K. J. Park, J. H. Lee, and Y. C. Chung, “OSNR monitoring technique based on orthogonal delayed-homodyne method,” *IEEE Photonics Technol. Lett.*, vol. 14, no. 10, pp. 1469–1471, 2002.

[44] C. Xie, D. C. Kilper, L. Möller, and R. Ryf, “Orthogonal-polarization heterodyne OSNR monitoring insensitive to polarization-mode dispersion and nonlinear

polarization scattering," *J. Light. Technol.*, vol. 25, no. 1, pp. 177–183, 2007.

[45] W. Chen, R. S. Tucker, X. Yi, W. Shieh, and J. S. Evans, "Optical signal-to-noise ratio monitoring using uncorrelated beat noise," *IEEE Photonics Technol. Lett.*, vol. 17, no. 11, pp. 2484–2486, 2005.

[46] X. Tian *et al.*, "Nonlinearity-Tolerant In-band OSNR Monitoring for Synchronous Traffic Using Gated-Signal RF Spectral Analysis," *Lightwave*, vol. 1, no. c, pp. 2–4, 2006.

[47] J. H. Lee, N. Yoshikane, T. Tsuritani, and T. Otani, "In-band OSNR monitoring technique based on link-by-link estimation for dynamic transparent optical networks," *J. Light. Technol.*, vol. 26, no. 10, pp. 1217–1225, 2008.

[48] J. H. Lee, H. Guo, T. Tsuritani, N. Yoshikane, and T. Otani, "Field trial of all-optical networking controlled by intelligent control plane with assistance of optical performance monitors," *J. Light. Technol.*, vol. 27, no. 2, pp. 94–100, 2009.

[49] N. Hanik, A. Gladisch, C. Caspar, and B. Strebel, "Application of Amplitude Histograms to Monitor Performance of Optical Channels," *Electron. Lett.*, vol. 35, no. 5, pp. 403–404, 1999.

[50] R. S. Luis, L. Costa, A. Teixeira, and P. André, "Optical performance monitoring based on asynchronous amplitude histograms," in *Optical Performance Monitoring*, C. C. K. Chan, Ed. Elsevier, 2010, pp. 145–174.

[51] R. Luis, A. Teixeira, and P. Monteiro, "Optical Signal-to-Noise Ratio Estimation Using Reference Asynchronous Histograms," *J. Light. Technol.*, vol. 27, no. 6, pp. 731–743, 2009.

[52] I. Shake, H. Takara, K. Uchiyama, and Y. Yamabayashi, "Quality monitoring of optical signals influenced by chromatic dispersion in a transmission fiber using averaged Q-factor evaluation," *IEEE Photonics Technol. Lett.*, vol. 13, no. 4, pp. 385–387, 2001.

[53] I. Shake, W. Takara, S. Kawanishi, and Y. Yamabayashi, "Optical signal quality monitoring method based on optical sampling," *Electron. Lett.*, vol. 34, no. 22, pp. 2152–2154, 1998.

[54] Z. Dong, F. N. Khan, Q. Sui, K. Zhong, C. Lu, and A. P. T. Lau, "Optical Performance Monitoring: A Review of Current and Future Technologies," *J. Light. Technol.*, vol. 34, no. 2, pp. 525–543, 2016.

[55] Z. Dong *et al.*, "Optical performance monitoring in DSP-based Coherent Optical Systems," in *Optical Fiber Communication Conference 2015*.

[56] M. S. Faruk and K. Kikuchi, "Monitoring of Optical Signal-to-Noise Ratio using Statistical Moments of Adaptive-Equalizer Output in Coherent Optical Receivers," *Opto-Electronics Commun. Conf.*, vol. 0, no. 7, pp. 233–234, 2011.

[57] C. Do, A. V. Tran, C. Zhu, D. Hewitt, and E. Skafidas, "Data-aided OSNR estimation

for QPSK and 16-QAM coherent optical system," *IEEE Photonics J.*, vol. 5, no. 5, 2013.

[58] R. Schmogrow *et al.*, "Error Vector Magnitude as a Performance Measure for Advanced Modulation Formats," *IEEE Photonics Technol. Lett.*, vol. 24, no. 1, pp. 61–63, 2012.

[59] Z. Dong, A. P. T. Lau, and C. Lu, "OSNR monitoring for QPSK and 16-QAM systems in presence of fiber nonlinearities for digital coherent receivers," *Opt. Express*, vol. 20, no. 17, 2012.

[60] H. G. Choi, J. H. Chang, H. Kim, and Y. C. Chung, "Nonlinearity-Tolerant OSNR Estimation Technique for Coherent Optical Systems," *Opt. Fiber Commun. Conf. 2015*, pp. 4–6.

[61] C. C. Do, C. Zhu, and A. V. Tran, "Data-Aided OSNR Estimation using Low-Bandwidth Coherent Receivers .," *IEEE Photonics Technol. Lett.*, vol. 26, no. 13, pp. 1291–1294, 2014.

[62] S. Perrin, "Bringing Disaggregation to Transport Networks," *Heavy reading, Fujitsu*, 2015.

[63] J. Donovan, "Hitting the Open Road: Software-Accelerating Our Network with Open Source," *AT&T Innovation Blog*, 2015. [Online]. Available: https://about.att.com/innovationblog/061714hittingtheopen.

[64] J. M. Fàbrega, M. Svaluto Moreolo, and L. Nadal, "Optical Performance Monitoring Systems in Disaggregated Optical Networks," 2018, pp. 1–4.

[65] M. De Leenheer, T. Tofigh, and G. Parulkar, "Open and Programmable Metro Networks," *Opt. Fiber Commun. Conf. 2016*, pp. 3–5.

[66] E. Riccardi, P. Gunning, O. S. G. L. De Dios, M. Quagliotti, V. Lopez, and A. Lord, "An Operator view on the Introduction of White Boxes into Optical Networks," *J. Light. Technol.*, vol. 36, no. 15, pp. 3062–3072, 2018.

[67] N. Sambo, K. Christodoulopoulos, A. Nikos, P. Giardina, C. Delezoide, and A. Sgambelluri, "Experimental demonstration of white box including different transponders and monitors , controlled by NETCONF and YANG," in *OFC 2018*, 2018, pp. 2–4.

[68] L. Velasco *et al.*, "Building Autonomic Optical Whitebox-Based Networks," *J. Light. Technol.*, vol. 36, no. 15, pp. 3097–3104, 2018.

[69] D. Kilper, "Dis-Aggregation as a Vehicle for Hyper-Scalability in Optical Networks," in *ONDM 2018*.

8 GANTT CHART

Gantt Chart
Research Proposal Timeline

Project Name	Project Duration	Start date	End Date	
ONFIRE	35 Months	14-May-18	31-Mar-21	CTTC, Spain / Nokia Bell Labs, Germany

Task ID	Task Description	Task Duration (Months)	Start Date (Month-Year)	End Date (Month-Year)	8 May-18	9 Jun-18	10 Jul-18	11 Aug-18	12 Sep-18	13 Oct-18	14 Nov-18	15 Dec-18	16 Jan-19	17 Feb-19	18 Mar-19	19 Apr-19	20 May-19	21 Jun-19	22 Jul-19	23 Aug-19	24 Sep-19	25 Oct-19	26 Nov-19	27 Dec-19	28 Jan-20	29 Feb-20	30 Mar-20	31 Apr-20	32 May-20	33 Jun-20	34 Jul-20	35 Aug-20	36 Sep-20	37 Oct-20	38 Nov-20	39 Dec-20	40 Jan-21	41 Feb-21	42 Mar-21
1.1	Study of the state of the art on disaggregated optical networks, low margin optical networks and optical performance monitoring techniques	6	May-18	Oct-18																																		
2.1	Investigation of novel performance monitoring techniques agnostic to the optical transmission waveforms	6	Sep-18	Feb-19																																		
2.2	Analysis and assessment of the proposed non-intrusive optical performance monitoring system deployed at the network nodes	3	Jan-19	Mar-19																																		
3.1	Study and deployment of elastic interfaces and programmable optical white boxes	11	Mar-19	Jan-20																																		
4.1	Study and design of flexible, programmable and modular transmission technologies/solutions for coping with zero margin operation	9	Oct-19	Jun-20																																		
5.1	Integration of the studied/proposed data plane solutions with control, orchestration and management planes, including selection of optimal approach for data and control plane interworking	3	Jul-20	Sep-20																																		
5.2	Demonstration of disaggregated network elements in ALUD experimental network facilities	2	Oct-20	Nov-20																																		
6.1	Thesis preparation and submission	4	Dec-20	Mar-21																																		